AD-A091 986 CASDE CORP TORRANCE CA F/G 6/7
INFLATABLE LIFERAFT STABILITY STUDY.(U)
SEP 79 F J NICKELS DOT-CG-817775-A
UNCLASSIFIED USCG-D-81-79 NL

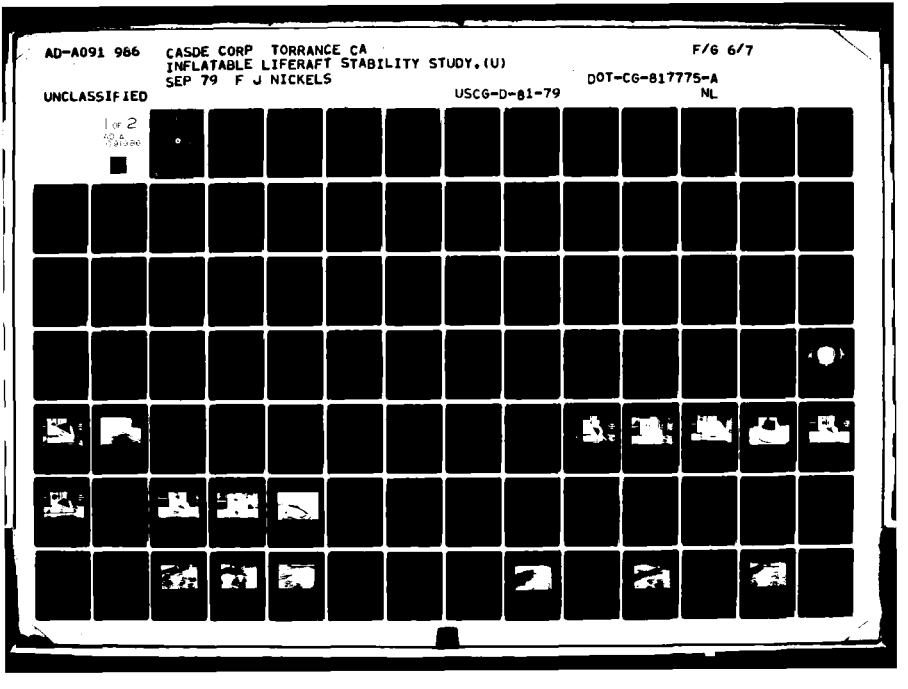

Report No. CG-D-81-79

LEVEL II

12 mc

INFLATABLE LIFERAFT STABILITY STUDY

SEPTEMBER 1979

FINAL REPORT

Prepared for

U.S. DEPARTMENT OF TRANSPORTATION
United States Coast Guard
Office of Research and Development
Washington, D.C. 20590

METRIC CONVERSION FACTORS

Approximate Conversions to Metric Measures

Symbol	When You Know	Multiply by	To Find	Symbol
		LENGTH		
in	inches	*2.5	centimeters	cm
ft	feet	30	centimeters	cm
yd	yards	0.9	meters	m
mi	miles	1.6	kilometers	km
		AREA		
in^2	square inches	6.5	square centimeters	cm^2
ft^2	square feet	0.09	square meters	m^2
yd^2	square yards	0.8	square meters	m^2
mi^2	square miles	2.6	square kilometers	km^2
	acres	0.4	hectares	ha
		MASS (weight)		
oz	ounces	28	grams	g
lb	pounds	0.45	kilograms	kg
	short tons (2000 lb)	0.9	tonnes	t
		VOLUME		
tsp	teaspoons	5	milliliters	ml
Tbsp	tablespoons	15	milliliters	ml
fl oz	fluid ounces	30	milliliters	ml
c	cups	0.24	liters	l
pt	pints	0.47	liters	l
qt	quarts	0.95	liters	l
gal	gallons	3.8	liters	l
ft^3	cubic feet	0.03	cubic meters	m^3
yd^3	cubic yards	0.76	cubic meters	m^3
		TEMPERATURE (exact)		
°F	Fahrenheit temperature	5/9 (after subtracting 32)	Celsius temperature	°C

*1 in = 2.54 (exactly). For other exact conversions and more detailed tables, see NBS Misc. Publ. 286, Units of Weights and Measures, Price $2.25, SD Catalog No. C13.10:286.

Approximate Conversions from Metric Measures

Symbol	When You Know	Multiply by	To Find	Symbol
		LENGTH		
mm	millimeters	0.04	inches	in
cm	centimeters	0.4	inches	in
m	meters	3.3	feet	ft
m	meters	1.1	yards	yd
km	kilometers	0.6	miles	mi
		AREA		
cm^2	square centimeters	0.16	square inches	in^2
m^2	square meters	1.2	square yards	yd^2
km^2	square kilometers	0.4	square miles	mi^2
ha	hectares (10,000 m^2)	2.5	acres	
		MASS (weight)		
g	grams	0.035	ounces	oz
kg	kilograms	2.2	pounds	lb
t	tonnes (1000 kg)	1.1	short tons	
		VOLUME		
ml	milliliters	0.03	fluid ounces	fl oz
l	liters	2.1	pints	pt
l	liters	1.06	quarts	qt
l	liters	0.26	gallons	gal
m^3	cubic meters	35	cubic feet	ft^3
m^3	cubic meters	1.3	cubic yards	yd^3
		TEMPERATURE (exact)		
°C	Celsius temperature	9/5 (then add 32)	Fahrenheit temperature	°F

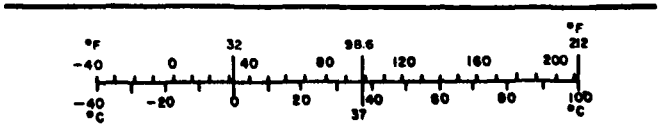

NOTICE

This document is disseminated under the sponsorship of the Department of Transportation in the interest of information exchange. The United States Government assumes no liability for its contents or use thereof.

The contents of this report do not necessarily reflect the official view or policy of the Coast Guard; and they do not constitute a standard, specification, or regulation.

This report, or portions thereof may not be used for advertising or sales promotion purposes. Citation of trade names and manufacturers does not constitute endorsement or approval of such products.

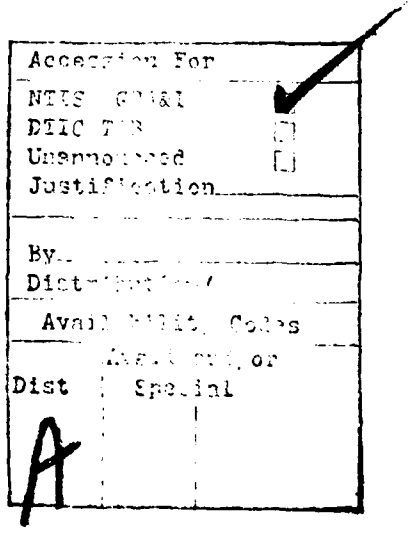

Technical Report Documentation Page

1. Report No.	2. Government Accession No.	3. Recipient's Catalog No.
USCG-D-81-79	AD-A094 986	

4. Title and Subtitle	5. Report Date
Study of Inflatable Liferaft Stability Study.	September 1979
	6. Performing Organization Code
	8. Performing Organization Report No. 12-197

7. Author(s)	10. Work Unit No. (TRAIS)
F.J. Nickels	

9. Performing Organization Name and Address	11. Contract or Grant No.
CASDE Corporation 2707 Toledo Street, Suite 604 P.O. Box 1291 Torrance, CA 90505	DOT-CG-817775-A New

12. Sponsoring Agency Name and Address	13. Type of Report and Period Covered
Department of Transportation U.S. Coast Guard Office of Research and Development Washington, D.C. 20590	Final Report July 1978 - September 1979
	14. Sponsoring Agency Code G-DSA-1/TP44

15. Supplementary Notes

The U.S. Coast Guard Office of Research and Development's technical representative for the work performed herein was Lieutenant J.C. Burson.

16. Abstract

This study was initiated to develop a framework for the evaluation of the general principles of inflatable liferaft stability and within that framework to evaluate the various concepts for stability enhancement. A Quasi-Static Inflatable Liferaft Stability Model was developed to evaluate the stability due to static effects; the analysis of dynamic effects was deferred to a later study; the procedure used is analagous to the evaluation of ship stability.

Wind tunnel tests were conducted to determine drag, lift, and moment coefficients as functions of pitch angle and bottom exposure. Model basin tests were also conducted. The stability Model was used to produce curves of net righting (or heeling) moment. The study was conducted for a flat bottom liferaft as well as for those with ballast pockets, a toroidal ballast bag, and a hemispherical ballast bag.

17. Key Words	18. Distribution Statement
Inflatable Liferaft Liferaft Stability Quasi-Static Stability Liferaft Stability Enhancement	Document is available to the public through the National Technical Information Service, Springfield, Virginia 22151

19. Security Classif. (of this report)	20. Security Classif. (of this page)	21. No. of Pages	22. Price
Unclassified	Unclassified	97	

Form DOT F 1700.7 (8-72) Reproduction of completed page authorized

411267

PREFACE

This report summarizes work conducted under Contract No. DOT-CG-817775-A by CASDE Corporation under the auspices of the U.S. Coast Guard with Lieutenant J.C. Burson serving as the Office of Research and Development's technical representative for the work performed herein. The program manager was Dr. R. Saucedo. Mr. F.J. Nickels was the principal investigator.

TABLE OF CONTENTS

LIST OF ILLUSTRATIONS

LIST OF ILLUSTRATIONS (Continued)

LIST OF ILLUSTRATIONS (Continued)

1.0 INTRODUCTION

The susceptibility of inflatable liferafts to capsizing when they are often the most needed, i.e. in high seas and/or winds, is well known from both operational experience (Reference 1) and experiment (References 2 and 3). Reference 2 documents the tendency of inflatable liferafts to capsize under the influence of high wind alone while Reference 3 suggests the possibility that even liferafts which have been designed to have a high degree of stability can be capsized in breaking waves.

Although inflatable liferafts have been employed on a supplemental basis in the past, their future potential use as primary group survival equipment necessitates a better understanding of their limitations with respect to stability, and potential measures for enhancing stability. Several concepts for a stability enhancement of inflatable liferafts have been placed on the market and these require objective evaluation.

1.1 Summary

The present study was initiated to develope a framework for the evaluation of the general principles of inflatable liferaft stability and within that framework to evaluate the various concepts for stability enhancement.

The study, as originally conceived, called for a program of tests of various liferaft configurations to determine relative stability merits. But tests provide isolated data points which are unique to the configuration tested and the test conditions and in themselves, if they are model tests, do not provide any enlightment to the nature of scale effects.

At the outset of the study, it was recognized that there are on the one hand dynamic wave (particularly breaking wave) forces and liferaft inertial forces and on the other hand comparatively static forces such as wind loads and buoyant forces which contribute to the stability of a liferaft in a particular circumstance. The analysis of dynamic effects were deferred, at least from the present study except as they manifest themselves in model testing.

On these considerations, a Quasi-Static Inflatable Liferaft Stability Model was developed which evaluates the stability of the liferaft due to static effects, only, as the liferaft is placed in a series of positions which would be due to dynamic response. The procedure is analogous to the evaluation of ship stability as it has evolved in the last ten years or so.

The Quasi-Static Stability Model first determines the condition of vertical force equilibrium of the liferaft at a given value of pitch angle and load. The four vertical force componants are the liferaft weight, buoyant force, water ballast weight and wind lift force. After the vertical equilibrium of these forces has been determined, the net righting (or heeling) moment is next determined.

Wind forces, particularly the lift force, were expected to be strongly dependent upon the pitch angle and the amount of bottom exposure (which is the same as specifying the angle and the buoyant volume). Wind forces and moments in the Quasi-Static Model are expressed as functions of coefficients which are in turn expressed as functions of pitch angle and percent of bottom diameter exposed (or conversely, immersed). Since such coefficients are not available in the aerodynamic literature, wind tunnel tests were conducted at the California Institute of Technology low speed wind tunnel on a three foot diameter rigid model of a circular planform liferaft with a closed canopy.

In the Quasi-Static Stability Model, the weight of water in free flooding ballast bags or pockets is not considered part of the weight of the liferaft nor is the volume of the ballast bag considered part of the buoyant force, since as long as the ballast bag or pocket is below the surface, these are self compensating. Only when a portion of the volume of a ballast bag is lifted above the water surface does the ballast become effective as it now provides weight but not buoyancy. Compensatory buoyancy is, of course, provided by the requirement for a vertical force balance which requires that the raft sink deeper in the water as ballast weight is lifted out of the water.

The Quasi-Static Model has routines to calculate the ballast forces and moments due to four quadrentally arranged ballast pockets (per current U.S.C.G. regulations), toroidal ballast bags of various depths and thicknesses, and hemispherical ballast bags of various radii. The outputs of the model (which has been,

computerized) are curves of net righting (or heeling) moment versus pitch angle and the areas under these curves.

The calculation of the righting moment under quasi-static conditions is not, of itself, a complete measure of stability of a liferaft, since the raft must survive in a dynamic environment. A three foot and a one and one half foot diameter model of a circular planform liferaft were tested in irregular seas with the significant wave heights up to 90 percent of the raft diameter and in actual winds of 19 knots. The tendency of the raft model with various stability enhancement devices to capsize was compared against the stability characteristics as calculated by the Quasi-Static Model. Conclusions relative to the ability of the Quasi-Static Model to determine a true measure of liferaft stability, an adequate measure of stability to avoid capsizing, and the relative performance of stability enhancing devices were drawn from the comparisons.

2.0 CONCLUSIONS AND RECOMMENDATIONS

The program was successful in meeting most of the objectives. Restructuring of the program from a purely test program to a program of analysis and test and expansion of the testing from solely wave tank testing to wave tank and wind tunnel testing necessitated the deletion of some areas of investigation from the study so that the expanded program could be accommodated within the same budget. Overall, the objectives of the Coast Guard have been met in that there now exists an objective basis for the evaluation of inflatable liferaft stability and a framework for structuring further studies and tests. Response to specific objectives is as follows:

1) Liferaft stability was investigated; towing response and maneuverability were not.
2) The effectiveness of ballast pockets, toroidal ballast bags, and hemispherical ballast bags in improving liferaft stability was evaluated. An attempt to evaluate the effectiveness of a skirt by testing failed. No attempt was made to evaluate the effectiveness of sea anchors because these are dynamic devices and therefore cannot be analyzed by the Quasi-Static Inflatable Liferaft Stability Model.
3) Procedures for testing inflatable liferaft models in wind and irregular long crested waves has been established as an effective procedure for testing the stability performance of inflatable liferafts.
4) The results of the wave tank and wind tunnel tests and the results of analysis with the Quasi-Static Model contained herein provide preliminary data for the development of performance criteria and performance test procedure for inflatable liferafts.
5) The determination of a standardized measure of stability by means of the Quasi-Static Inflatable Liferaft Stability Model and its evaluation by comparison with a stability criterion is offered as a potential basis on which the Coast Guard should evaluate new or unusual liferaft designs for approval.
6) On the basis of the results of this study, toroidal and hemispherical ballast bag configurations provide such large improvements in resistance to capsizing over unballasted or ballast pocket configurations that their mandatory use should be considered.

2.1 Conclusions

The conclusions that can be drawn from this study are as follows:

a) The results of analysis with the Quasi-Static Inflatable Liferaft Stability Model and the wind tunnel test coefficients show that moderate wind speeds can cause flat bottom inflatable liferafts to be picked up and overturned when their bottoms become exposed due to pitch motion.

b) Model tests in rough seas and moderate winds did not corroborate the conclusion in (a) because even the steepest seas generated (provided the crests do not break) did not cause the bottom to become exposed.

c) It is uncertain whether capsizing would occur in the same sea conditions with higher wind speeds than were available at the test facility although the capsizings that were produced in the Elizabeth City tests (Reference 2) in zero sea state and high winds would indicate that the Quasi-Static Model results are correct.

d) Model tests indicate that dynamic forces in breaking waves are at least as potent in causing liferaft capsizing as wind forces.

e) Ballast pockets per U.S.C.G. requirements provide about 50 percent more calculated static stability than liferafts without ballast but were demonstrated to have little effect in preventing capsizing in the model tests.

f) Both toroidal ballast bags and hemispherical ballast bags were demostrated to be 100 percent effective in preventing capsizing in the wind and wave conditions available for the model tests.

g) Both toroidal ballast bags and hemispherical ballast bags demonstrated a very high natural pitch frequency which would be likely to give a very rough ride to survivors.

h) The toroidal ballast bag provided slightly higher righting moments than the hemispherical ballast bag through-out the first 30 degrees of pitch angle while carrying only 50 percent of the weight of ballast water.

i) The righting moment of the toroidal ballast bag would be approximately equal to the hemispherical ballast bag if the width of the toroidal ballast bag were halved so as to contain only 25 percent of the weight of the hemispherical ballast bag.

2.2 Recommendations

A major result of this study is the demonstration that consideration of solely static effects is insufficient for establishing stability criteria or for evaluating total stability characteristics of inflatable liferafts. The model test results show that the effect of breaking waves can be as significant a factor in liferaft stability as wind forces. While the effects of aero- and hydrostatic forces have been thoroughly evaluated in this report, the mechanics of instability in breaking waves are poorly understood. Thus it is essential that the dynamic performance of liferafts in breaking waves be studied before a comprehensive criterion for liferaft stability can be formulated and before a methodology for evaluating the stability of a liferaft can be developed. In addition because of the limitations of the available equipment at the towing tank, model tests have not been conducted in extreme enough wind and sea conditions to fully verify the Quasi-Static Inflatable Liferaft Stability Model for the complete range of liferaft operating conditions.

It is therefore recommended that additional studies be performed of liferaft stability in breaking waves and to extend the model tests to more extreme wind and sea conditions. Circular planform inflatable liferafts are not unlike the USCG's "monster" navigational buoys in hydrodynamic behavior. A study of the capsizing tendency of the "monster" buoy in breaking waves was reported in Reference 4. The method of analysis used in that report can be applied to the problem of inflatable liferaft stability in waves. It is recommended that such a study be carried out with the use of the computer program contained in Reference 4. The study would involve analysis of inflatable liferafts with alternative stability enhancement features to determine the effect of liferaft characteristics, including amount and configuration of ballast, on stability in breaking waves. Although there are deficiencies in the state of the art particularly with regard to nonlinearities in the hydrodynamic effects which limit the accuracy of such

analysis, the relative stability of alternative configurations should be correctly determined. The results should be verified by model testing which will also involve the development of a test technique for generating consistent breaking waves with measurable characteristics.

On the basis of the test conducted to date, the size of the wave appears not to be a factor in liferaft capsizing. In fact, longer waves (provided they do not break) seem to be easier for a liferaft to survive. Therefore, the length of the waves in higher sea states than were generated in the present tests probably would not produce different results. Nevertheless this should be verified and it is recommended that the liferaft model be tested in higher sea states (say to sea state 8) by means of smaller scale models at Offshore Technology Corporation or with the same models at a facility capable of generating higher waves. Tests with a smaller model would also provide an opportunity to study the effect of scale factor since tests could be made for the same sea state and wind velocity as were made with the eighteen inch diameter model.

Figure 7-3 of this report shows that, in three different conditions of wind and waves, there appears to be a common threshold value of calculated righting moment (at a particular pitch angle) at which the tendency to capsize begins. This righting moment is actually the net of the righting moments due to hydrostatic and ballast forces and the aerodynamic heeling moment. At the threshold of capsizing it is implied that it is equal to the uncalculated net heeling moment. If this (or some other) measure of the threshold of capsizing can be shown to be consistent over a complete range of liferaft operating conditions then it may be possible to utilize it (with a margin) as a criterion for liferaft stability. The basis for Coast Guard approval would then be the calculated value of the righting moment by some standardized calculation procedure such as the Quasi-Static Inflatable Liferaft Stability Model. This procedure is completely analogous to the Coast Guard's procedures for regulating the stability of merchant ships.

Before such a procedure can be implemented additional model tests must be made to ascertain whether the value of the calculated righting moment at the threshold of capsizing remains constant for the complete range of operating conditions for inflatable liferafts. Specifically, each liferaft configuration needs to be tested in much more severe wind and sea conditions — to scaled sea state 8 and 100 knot wind speeds, if possible. Higher sea states can be obtained by testing smaller scale models at Offshore Techology Corporation with the possibility of a deterioration in accuracy due to the small scale or by testing the current models at a facility with adequate wave generation capability. The problem of testing the models in higher wind speeds requires further study to determine the equipment required to create the required conditions.

3.0 STUDY APPROACH

The evaluation of inflatable liferaft stability in this report is based upon the standard approach used to evaluate ship stability. In that approach, the characteristics of the righting and heeling moments in still water are calculated. The stability is then evaluated with respect to stability criteria which are intended to ensure that a given measure of still water stability will also provide adequate stability in all conditions likely to be met at sea.

Confidence in this approach for ships has been achieved through years of correlation between calculated still water stability characteristics and actual experience at sea. (Recently there have also been attempts to calculate the dynamic stability of ships in a limited number of specific sea conditions.) There has been no requirement to demonstrate a measure of calculated still water stability for inflatable liferafts. As a result, there has been no body of standarized stability measure data with which to correlate whatever liferaft stability experience there exists. Hence there is no reliable stability criterion for liferafts. In fact there is no stability criterion at all.

In view of the above, the approach to the evaluation of stability of inflatable liferafts must include the development of a general methodology for calculating still water righting and heeling moment curves and the correlation of the resulting calculated still water stability measures with observed performance at sea. This was accomplished in three steps:

1) development of a generalized quasi-static inflatable liferaft stability model,
2) wind tunnel testing to obtain the aerodynamic force and moment coefficients to be used in the model, and
3) wave tank tests to obtain some correlation between the calculated still water stability measure and performance at sea.

There is one significant difference between the stability characteristics of ships and inflatable liferafts when the heeling moment is imposed by wind that requires a somewhat different approach to analysis. It is customary in the analysis of stability of ships to ignore any vertical componant of the wind force. At any angle of heel, buoyancy is assumed to be exactly equal to the weight of the ship.

Thus, the righting moment provided by the buoyant force can be calculated independently of the heeling moment produced by the wind.

The vertical component of the wind force is often significant on inflatable liferafts and cannot be ignored. A large vertical component of wind force generated when the flat bottom of raft is exposed to the wind will tend to lift the raft and reduce the buoyant force. It is therefore meaningless to attempt to decouple the heeling and righting moments. It is only possible to calculate the net righting (or heeling) moment; the sign of the moment determines which it is.

It is generally considered adequate in the analysis of ship stability to assume that the ship rotates about an axis through the center of gravity, although this is not strictly true. It is certainly not true for flat bottomed, unballasted inflatable rafts under the influence of significant wind forces since the center of gravity undergoes vertical and horizontal translations. In the method of analysis used in this study, the rotational moments are calculated for the condition where the raft is in vertical equilibrium and at a given pitch angle. This implies that the displaced volume remains constant and that the center of buoyancy remains approximately fixed. Thus an appropriate assumption is that the raft rotates about the center of buoyancy.

4.0 QUASI-STATIC INFLATABLE LIFERAFT STABILITY MODEL

A quasi-static stability model has been developed to provide a standard method for determining the stability characteristics of various configurations of inflatable liferafts. The model consists of a system of equations and a procedure for solving them. In this respect it is somewhat analogous to the "added weight" and "lost buoyancy" methods of damaged stability analysis for ships.

The output of the model is the curve of net righting moment versus heel (or pitch) angle for the liferaft afloat in still water in a uniform wind. The model is called quasi-static because it computes only the static forces and moments acting on the liferaft in a situation where, in general, dynamic forces would also be acting upon it. That is, if a liferaft were, at any instant, poised at a particular pitch angle and vertical position and there were a net moment acting upon it, the raft would not be in equilibrium and would be undergoing translation and rotation. The value of such an analysis, incomplete though it may be, is that it evaluates the potential of the static forces and moments to overcome whatever dynamic capsizing effects may occur.

There are four static forces considered to act on the liferaft in the quasi-static stability model: 1) the liferaft weight exclusive of water ballast, W, 2) the buoyancy exclusive of the effect of water ballast bags, B, 3) the water ballast weight, BA, and 4) the resultant wind force, R_W. These forces and their moment arms abouts the center of buoyancy are shown in Figure 4-1. The moment about the center of buoyancy, M_B, is:

$$M_B = W \cdot \overline{GZ} + BA \cdot ba - R_W \cdot b$$

where:

$\overline{GZ}$ = horizontal distance between the lines of action of W and B
ba = horizontal distance between the lines of action of BA and B
b = distance perpendicular to line of action of resultant wind force to the center of buoyancy.

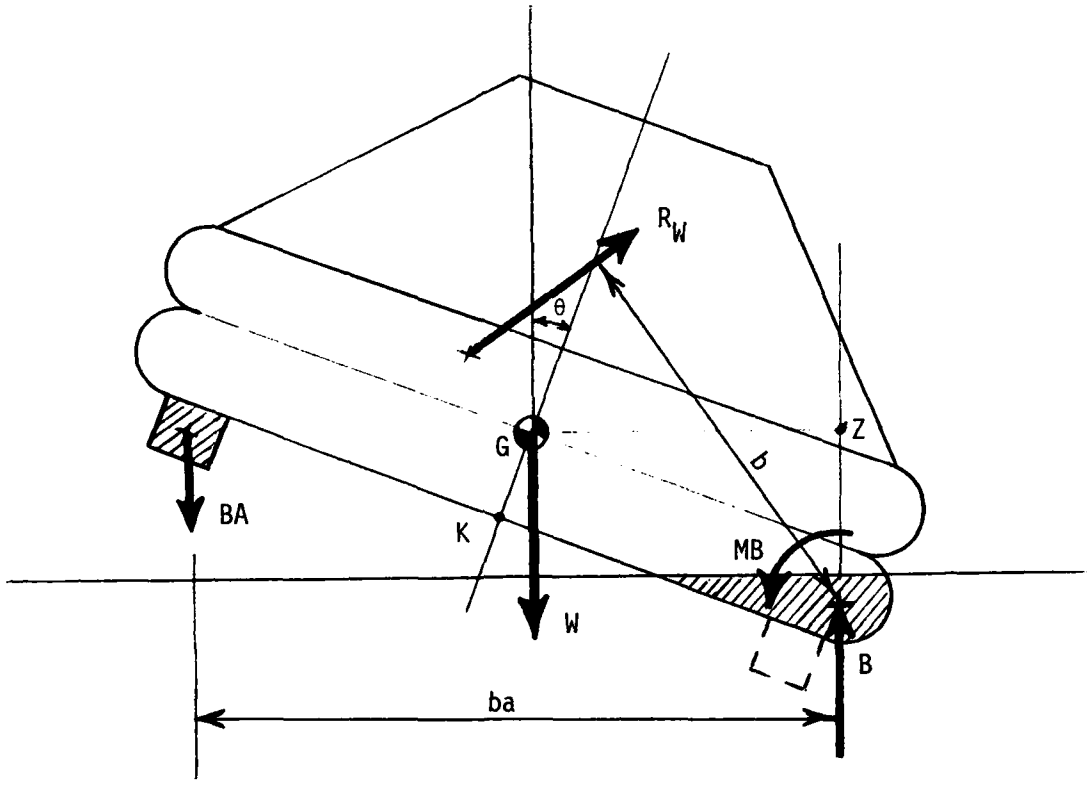

FIGURE 4-1

FORCE AND MOMENT DESCRIPTIONS FOR

QUASI-STATIC INFLATABLE LIFERAFT STABILITY MODEL

In this model the submerged portions of free flooding ballast bags are neglected altogether since the static buoyancy and weight forces and their moments exactly compensate each other. (This is not true of dynamic forces and moments induced by the ballast bags.) Thus, buoyant forces are solely those due to the inflated tubes of the raft and ballast weights are only those generated by the portion of the ballast bag which emerges from the water when the raft pitches (or heels).

The weight of the liferaft is the weight of the basic raft with canopy (if fitted) and all equipment and people on board but not water ballast. It is assumed that all weights are arranged symmetrically about the central vertical axis. The vertical position of the center of gravity can be specified as a parameter of the model.

The resultant wind force is the resultant of the vertical (lift) and horizontal (drag) components which are estimated on the basis of wind tunnel test results.

Planform shape of a liferaft can be a factor in its stability. An oblong shaped raft will in general have higher stability when it heels about its long axis than when it heels about its short axis because the moment arms b, ba, and $\overline{GZ}$ will generally be greater in the former case. A free floating oblong liferaft will generally orient itself with its long axis parallel to the wave crests so that it is in the least stable orientation; however, with a sea anchor deployed it is sometimes possible to control raft heading so that it is in the more stable orientation.

The aspect ratio of an oblong planform liferaft will affect the degree to which stability can be increased through orientation control. Inclusion of this parameter in this study would confuse the issue of the extent to which water ballast applied in various configurations can enhance liferaft stability. The quasi-static stability model, as presently developed, is therefore based upon a circular planform raft. Conclusion drawn from use of the model with respect to the benefits of various water ballast bag configurations will be generally true for non-circular planforms as well.

The quasi-static inflatable liferaft stability model has been developed for four configurations of ballast bags as follows:

a) a basic raft comprised of two vertically stacked, inflated, toroidal tubes with a flat bottom tangent to the bottom tube,
b) the same configuration as (a) with four rectangular, free flooding ballast pockets arranged at the quadrants along and perpendicular to the axis of pitch rotation,
c) the same configuration as (a) with a toroidal, free flooding ballast bag suspended from the lower inflated tube; the ballast bag has a rectangular cross section, the outer diameter of the toroid being equal to the outer diameter of the raft,
d) the same configuration as (a) with a hemispherical free flooding ballast bag suspended from the flat bottom.

The flexibility inherent in the fabric inflated tubes and ballast bags of inflatable liferafts will cause distortions in the geometrical relationships shown in Figure 1 which will affect the stability of the liferaft. Such flexibility can vary considerably depending upon the structural design of the raft. No attempt has been made to account for flexibility in the present version of the quasi-static stability model; the geometry is considered to be completely rigid.

4.1 Buoyant Force and Moment

Since ballast bag buoyancy is excluded from the liferaft buoyancy in the model, the buoyant force, B, and its centroid can be expressed by common functions (of draft and pitch angle as well as raft dimensions) for all four configurations. The circular planform of the liferaft enables expression of the buoyancy characteristics by closed form mathematical expressions rather than the more common approach in naval architecture of numerical integration which would be tedious in this application. To accomplish this, the tubular liferaft shape is idealized as a shallow, wall sided cylinder. The diameter of the cylinder, D', is set so that the walls of the cylinder pass through the centroid of the outer semicircle of the liferaft tubes. Thus when the tube (with zero pitch angle) is one half or fully submerged, the displaced volume of the cylinder and the liferaft will be equal. At other drafts and when the liferaft is pitched (or heeled) there will be slight differences in volume. The relationship of the idealized cylinder diameter, D' to the raft dimensions is

$$D' = D - 0.58t$$

where

t = liferaft tube diameter

D = liferaft outer diameter

The immersed volume of the cylinder with diameter, D', inclined at angle θ, with the bottom partly emerged can be obtained by integration where the reference axis and limits of integration are as given in Figure 4-2. ($R' = D'/2$.)

The immersed volume, V, is obtained by integration as follows:

$$V = 2\int_0^{d'} y\, h\, dx$$

Since

$$h = (d' - x) \tan \theta$$

and

$$y = \mp \sqrt{2R'x - x^2}$$

then

$$V = 2 \tan \theta \int_0^{d'} (d' - x) \sqrt{2R'x - x^2}\, dx$$

which becomes

$$V = R'^3 \tan \theta \left\{ \left(\frac{d'}{R'} - 1\right)^2 \sqrt{2\,\frac{d'}{R'} - \left(\frac{d'}{R'}\right)^2} + \left(\frac{d'}{R'} - 1\right) \left[\sin^{-1}\left(\frac{d'}{R'} - 1\right) + \frac{\pi}{2}\right] + \frac{2}{3}\left[2\,\frac{d'}{R'} - \left(\frac{d'}{R'}\right)^2\right]^{\frac{3}{2}} \right\}$$

Similarly, the moment of the buoyant volume about the z axis, M_z, is obtained from the integration:

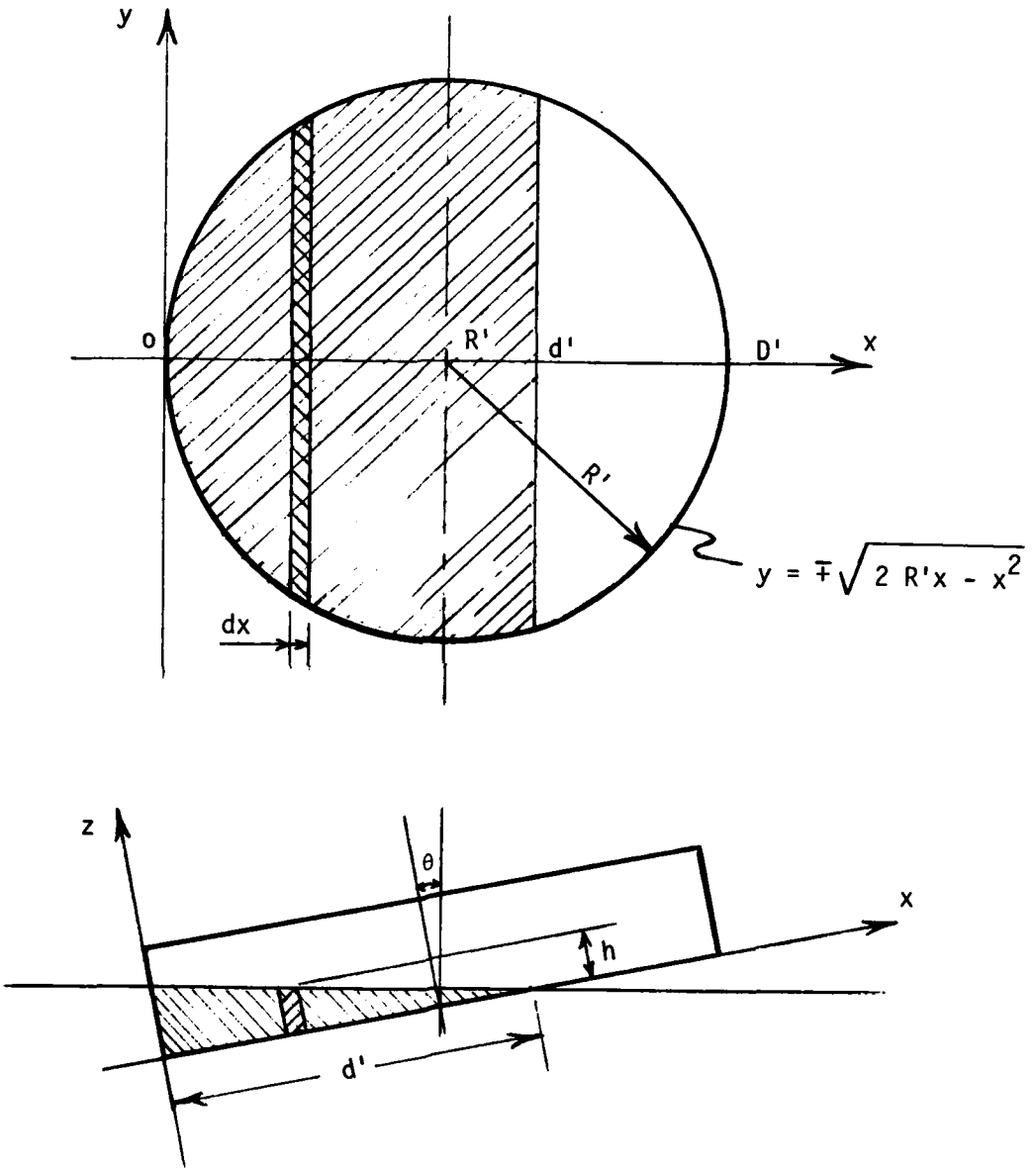

FIGURE 4-2

GEOMETRICAL RELATIONSHIPS FOR DETERMINING

DISPLACED VOLUME AND CENTER OF BUOYANCY OF

INFLATABLE LIFERAFT INCLINED AT ANGLE θ

$$M_z = 2 \int_0^{d'} x\ y\ h\ dx$$

thus

$$M_z = 2 \tan \theta \int_0^{d'} x\ (d' - x) \sqrt{2R'x - x^2}\ dx$$

which becomes

$$M_z = R'^4 \tan \theta \left\{ \left(\frac{d'}{R'} - \frac{5}{4} \right) \left[\left(\frac{d'}{R'} - 1 \right) \sqrt{2\,\frac{d'}{R'} - \left(\frac{d'}{R'} \right)^2} + \sin^{-1} \left(\frac{d'}{R'} - 1 \right) + \frac{\pi}{2} \right] + \frac{5 - \frac{d'}{R'}}{6} \left[2\,\frac{d'}{R'} - \left(\frac{d'}{R'} \right)^2 \right]^{\frac{3}{2}} \right\}$$

And the moment of the buoyant volume about the x axis, M_x, is obtained from a similar integration:

$$M_x = 2 \int_0^{d'} \frac{h}{2}\ y\ h\ dx$$

thus

$$M_x = \tan^2 \theta \int_0^{d'} (d' - x)^2 \sqrt{2R'x - x^2}\ dx$$

which becomes $$M_x = \frac{R'^4 \tan^2\theta}{2}\left\{\left[\frac{5}{4} - 2\frac{d'}{R'} + \left(\frac{d'}{R'}\right)^2\right]\left[\left(\frac{d'}{R'} - 1\right)\sqrt{2\frac{d'}{R'} - \left(\frac{d'}{R'}\right)^2} + \sin^{-1}\left(\frac{d'}{R'} - 1\right) + \frac{\pi}{2}\right] + \frac{5\left(\frac{d'}{R'} - 1\right)}{6}\left[2\frac{d'}{R'} - \left(\frac{d'}{R'}\right)^2\right]^{3/2}\right\}$$

The coordinates of the center of buoyancy about an axis system through the center of the liferaft, as shown in Figure 4-3, can then be obtained from:

$$\bar{z} = \frac{M_x}{V}$$

and

$$\bar{x} = R' - \frac{M_z}{V}$$

The moment arm of the weight about the center of buoyancy, $\overline{GZ}$, can then be obtained by geometry as:

$$\overline{GZ} = \bar{x}\cos\theta - (\overline{KG} - \bar{z})\sin\theta$$

The buoyant force, B, is obtained from:

$$B = w\,V$$

where

w = specific weight of water.

The first step in the computational procedure for the quasi-static inflatable liferaft stability model is to determine the equilibrium position of the raft at a given angle of pitch with no wind force. In this condition, the summation of vertical forces requires that:

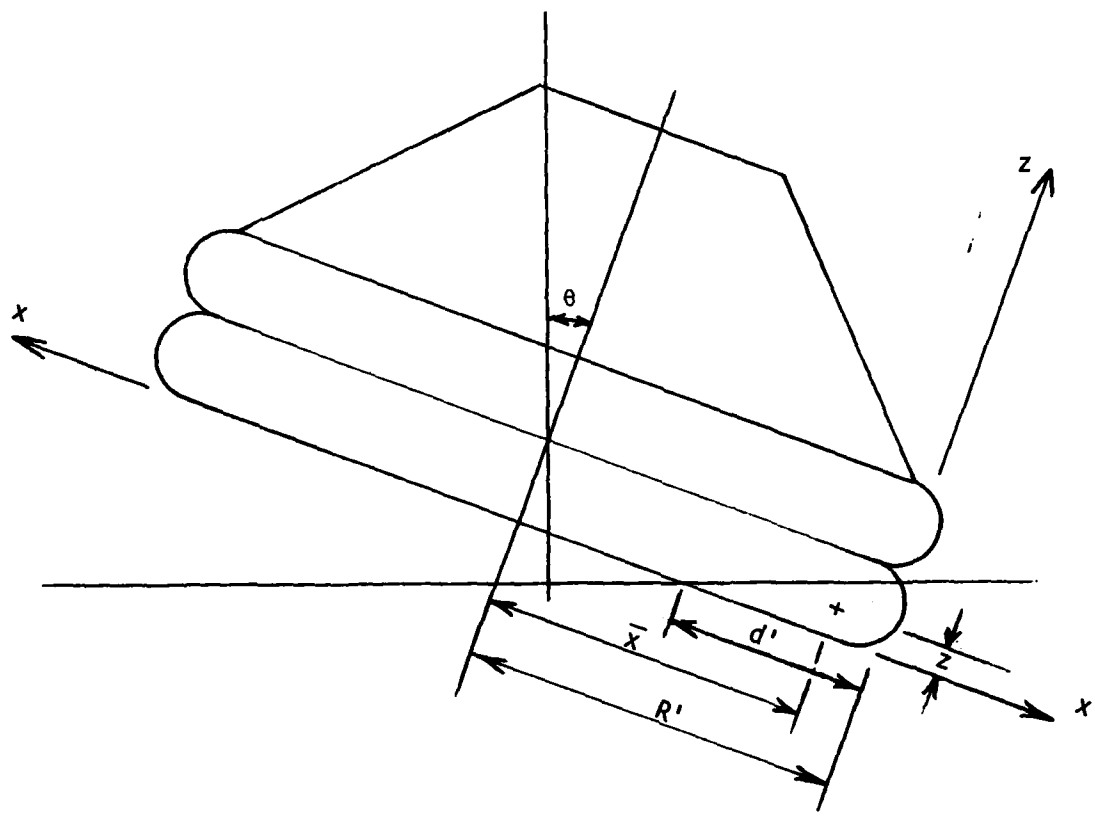

FIGURE 4-3

DESCRIPTION OF COORDINATES OF THE CENTER OF BUOYANCY

OF AN INFLATABLE LIFERAFT INCLINED AT ANGLE θ

$$V = \frac{W}{w}$$

In the computerized quasi-static stability model, the equation for the immersed volume, V, is solved iteratively to obtain the length of immersed bottom, d'. Alternatively, the equation for V (or V/tan θ) could be graphed to enable the value of d' to be read.

4.2 Wind Forces and Moment

With the quantities θ and d' known, the wind lift force, L, is next determined. Wind tunnel tests of models of each of the four configurations at various values of pitch angle, θ, and length of bottom immersion, d', were conducted to obtain lift, drag, and moment coefficients. The wind tunnel test results are presented as curves of lift, drag, and moment coefficients, C_L, C_D, and C_M, respectively, versus pitch angle, θ, and ratio of bottom immersion to liferaft diameter, d'/D, in Figures 5-19 through 5-21. The lift coefficient, C_L, for the value of pitch, θ, and length of immersed bottom, d', is read from Figure 5-19. The lift force, L, is calculated from

$$L = \rho/2 \; A \; C_L \; v^2$$

where

ρ = mass density of air

A = liferaft planform area $(= \pi \frac{D^2}{4})$

v = wind velocity

The next step in the procedure for the quasi-static inflatable liferaft stability model is to consider the effect of the wind lift force on reducing the buoyant force because

$$W = B + L$$

Thus, the displaced volume, V, is recalculated as

$$V = \frac{W - L}{w}$$

A revised length of immersed bottom is then obtained for this new value of displaced volume. The process of recalculating displaced volume and then wind lift force is repeated until the change in values from one calculation to the next becomes negligible (say less than one percent). At this point in the analysis, the liferaft is in vertical equilibrium.

It is possible that before the point of vertical equilibrium is reached, the lift force may grow to exceed the weight in which case the buoyant force would be reduced to zero. This represents the condition where the liferaft is blown completely out of the water. This condition has actually been observed at the Coast Guard's Elizabeth City, North Carolina liferaft stability tests. When the liferaft becomes completely airborne, there is no longer a center of buoyancy about which the raft can rotate and therefore the quasi-static stability model is not a valid method for evaluation of stability. The actual behavior of the raft after it leaves the water is likely to be very erratic and the raft may or may not capsize. Nevertheless becoming airborne is at least as precarious a situation as capsizing while afloat. Therefore, once the liferaft is airborne, it is not necessary to proceed to calculate righting moments to determine that the liferaft is unstable.

When the condition of vertical equilibrium has been defined, the wind drag and moment coefficients are read from the appropriate wind tunnel test result curves for the equilibrium value of immersed bottom length, d', and value of pitch angle, θ, being analyzed.

The wind drag force, D_W, and moment, M_W, are obtained from equations similar to that for the wind lift force, that is:

$$D_W = \rho/2 \; A \; C_D \; v^2$$

and

$$M_W = \rho/2 \; A \; R \; C_M \; v^2$$

where M_W is positive in the clockwise direction about the centroid of the liferaft buoyancy tubes as shown in Figure 4-4.

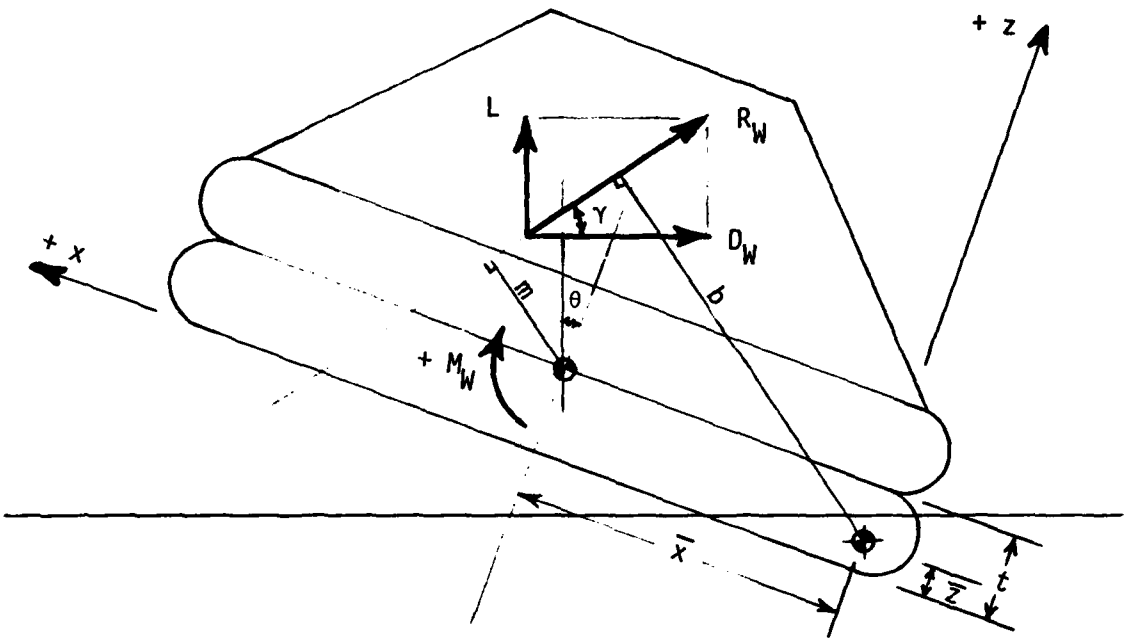

FIGURE 4-4

GEOMETRICAL DEFINITIONS OF WIND FORCES AND MOMENTS

ON AN INFLATABLE LIFERAFT INCLINED AT ANGLE θ

The resultant wind force, R_W, is found from the wind lift and drag forces, L and D_W, by

$$R_W = \sqrt{L^2 + D_W^2}$$

and its angle from the horizontal, γ, is

$$\gamma = \tan^{-1} \frac{L}{D_W}$$

The moment arm, m, of the resultant wind force, R_W, about the centroid of the liferaft is obtained from

$$m = \frac{M_W}{R_W}$$

Then, by geometry the moment arm, b, of the resultant wind force, R_W, about the center of buoyancy is expressed as:

$$b = \bar{x} \sin(\theta + \gamma) + m + (t - \bar{z}) \cos(\theta + \gamma)$$

4.3 Ballast Force and Moment

The remaining part of the quasi-static inflatable liferaft stability model is the determination of the ballast weight, BA, and its moment arm, ba, about the center of buoyancy, B. A separate method for calculating these quantities, is required for each of the four configurations considered in this report. The ballast weight BA, is the product of the specific weight of the water the liferaft is afloat in and the portion of the volume of the ballast bag which is above the water surface by the reason of the liferaft's pitch angle and wind induced lift. The ballast bag is assumed to be completely full. There is no consideration for loss of ballast water through the free flooding ports. Also, there is no consideration of any sagging which may reduce the moment arm of the ballast, that is, the ballast bags are assumed, for the mathematical model, to be completely rigid.

4.3.1 Flat Bottom

The flat bottom configuration has no water ballast, therefore

$$BA = 0$$

and there is no meaning to ba.

4.3.2 Ballast Pockets

The orientation of the four quadrantal ballast pockets has an influence upon the amount of ballast moment produced. When all of the ballast pockets are fully immersed the righting moment produced is the same whether the pockets are in an "X" or a "+" orientation. However in more usual conditions of load and pitch angle, one orientation may produce either more or less righting moment than another. (e.g., when the raft is heavily loaded the "+" orientation will produce the greatest righting moment since the two high side pockets of a "X" orientation may not emerge at all. On the other hand, in a partial load condition at high pitch angles, the two emerged pockets of an "X" orientation would produce more righting moment than the one emerged pocket of a "+" orientation since its moment arm would always be less than twice the other's.) In any case, the differences in righting moment due to ballast pocket orientation are of second order. For simplicity, the quasi-static stability model has been developed for only one orientation. The "+" orientation was selected.

The ballast weight, BA, is developed in two parts, BA1, and BA2, such that:

$$BA = BA1 + BA2$$

BA1 is the ballast weight of the single ballast pocket at the "bow" or the head of the "+". BA2 is the combined ballast weight of the two ballast pockets at the "beams amidships" or the "wings" of the "+". The moment arms for the two sets of ballast pockets are similarly designated ba1 and ba2 and the total moment arm of all ballast pockets, ba, is obtained from

$$ba = \frac{ba1 \cdot BA1 + ba2 \cdot BA2}{BA1 + BA2}$$

The calculation of the volume of ballast and its moment depends, (according to the mathematical procedures developed for this study) on whether the ballast pocket is completely out of the water or, if it is not, whether the water surface intersects the flat bottom of the pocket or not. Thus there are three possible computations of the ballast weight of a ballast pocket. To determine which computation is to be used, the distance perpendicular to the bottom of the liferaft to the water surface at the forward and aft ends of the ballast pockets are compared with the depth of the pocket. If at the after end the distance is greater than the depth of the pocket, then the pocket is entirely out of the water. If the distance at the forward end is less than the depth of the pocket, then the entire bottom of the pocket is in the water. It is assumed that, (in accordance with current practice) the outside of the pocket is situated under the center of the buoyancy tube. Referring to Figure 4-5, the width and length of the pocket are v and u, respectively.

For the pocket at the "bow" (or "head" of the "+") the perpendicular depths from the bottom of the raft to the water surface at the forward and aft sides of the pocket, designated q_1 and q_2, respectively, are:

$$q_1 = (D - d' - 0.79t) \tan \theta$$

and

$$q_2 = (D - d' - 0.79t - v) \tan \theta$$

If $q_2 > k$:

$$BA1 = w\ k\ u\ v$$

and

$$ba1 = \left[\bar{x} + \frac{D}{2} - \frac{t}{2} - \frac{v}{2} + \left(\bar{z} + \frac{k}{2}\right) \tan \theta\right] \cos \theta$$

If $q_1 < k$:

$$BA1 = w \left(\frac{q_1 + q_2}{2}\right) u\ v$$

and

$$ba1 = \left[\bar{x} + \frac{D}{2} - \frac{t}{2} - \frac{v}{2} + \left(\bar{z} + \frac{q_1 + q_2}{4}\right) \tan \theta\right] \cos \theta$$

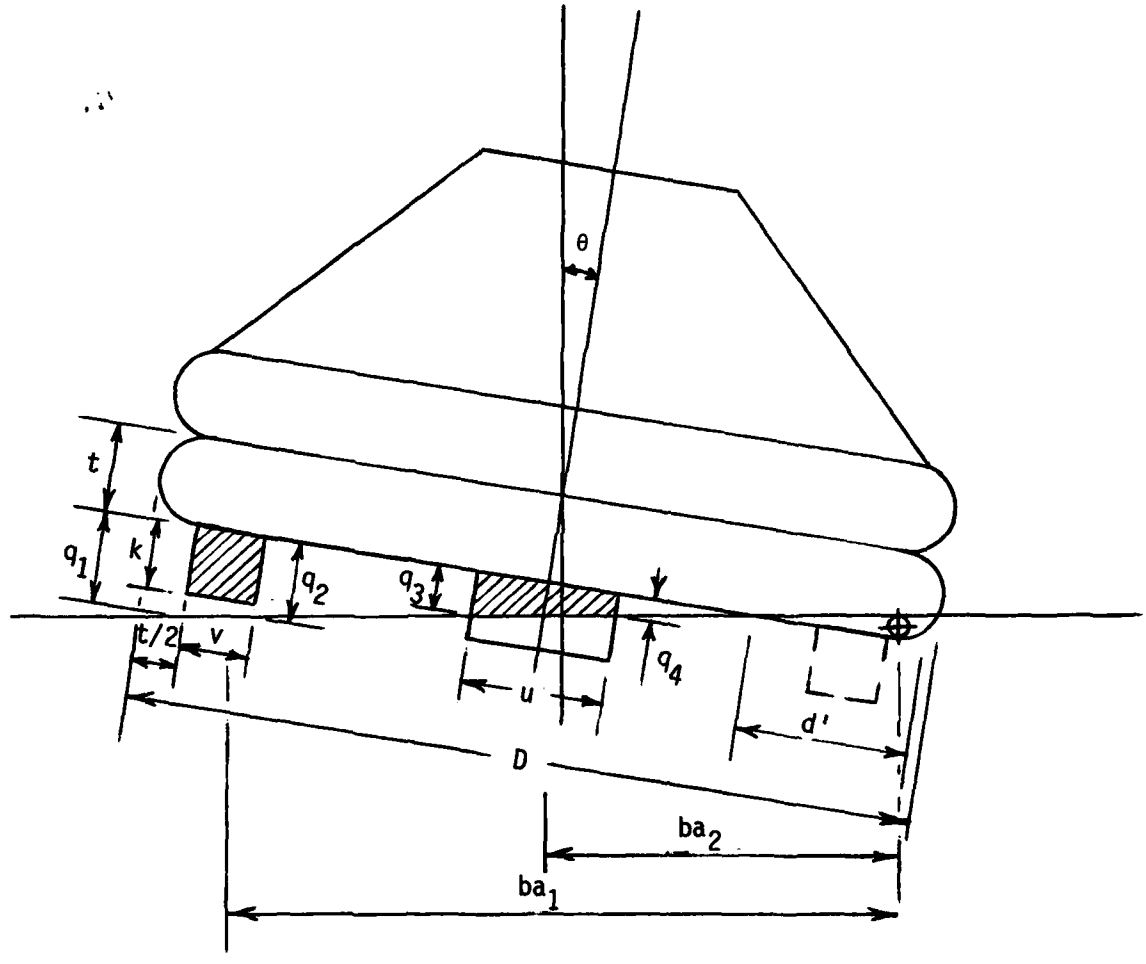

FIGURE 4-5

GEOMETRICAL RELATIONSHIPS FOR DETERMINING BALLAST

WEIGHT AND CENTER OF GRAVITY OF BALLAST POCKETS

If $q_2 < k$ and $q_1 > k$:

$$BA1 = w\,u\left[kv - \frac{(k - q_2)^2}{2\tan\theta}\right]$$

and

$$bal = \left[\bar{x} + \frac{D}{2} - \frac{t}{2} - \frac{v}{2} + \left(\bar{z} + \frac{k}{2}\right)\tan\theta\right]\cos\theta$$

Similarly, for the side ballast pockets:

$$q_3 = (0.5D - d' - 0.29t + \frac{u}{2}) \tan\theta$$

and

$$q_4 = (0.5D - d' - 0.29t - \frac{u}{2}) \tan\theta$$

If $q_4 > k$:

$$BA2 = 2\ w\ k\ u\ v$$

and

$$ba2 = \left[\bar{x} + (\bar{z} + \frac{k}{2}) \tan\theta\right] \cos\theta$$

If $q_3 < k$:

$$BA2 = 2w\ (\frac{q_3 + q_4}{2})\ u\ v$$

and

$$ba2 = \left[\bar{x} + (\bar{z} + \frac{q_3 + q_4}{2}) \tan\theta\right] \cos\theta$$

If $q_4 < k$ and $q_3 > k$: —

$$BA2 = 2\ w\ v\ \left[k\ u - \frac{(k - q_4)^2}{2 \tan\theta}\right]$$

and

$$ba2 = \left[x + (z + \frac{k}{2}) \tan\theta\right] \cos\theta$$

4.3.3 Hemispherical Ballast Bag

When a liferaft fitted with a hemispherical ballast bag pitches a segmental spherical wedge of ballast water rises above the water surface. The volume of this wedge of ballast water depends upon the radius of the ballast bag, GR, the pitch angle, θ, and the length of the immersed bottom, d'. The procedure developed for calculating the volume and moment of this wedge is to assume that it is equivalent to a wedge of a cylinder whose base is concentric with the base of the raft and that it has a diameter equal to the diameter of the mean circular section through the segmental circular wedge. The radius of this circle, GR2, is obtained by geometry with reference to the quantities shown in Figure 4-6, where:

$$r_1 = \frac{D}{2} - (d' + 0.29t)$$

$$r_2 = r_1 \cos(\frac{\theta}{2})$$

and

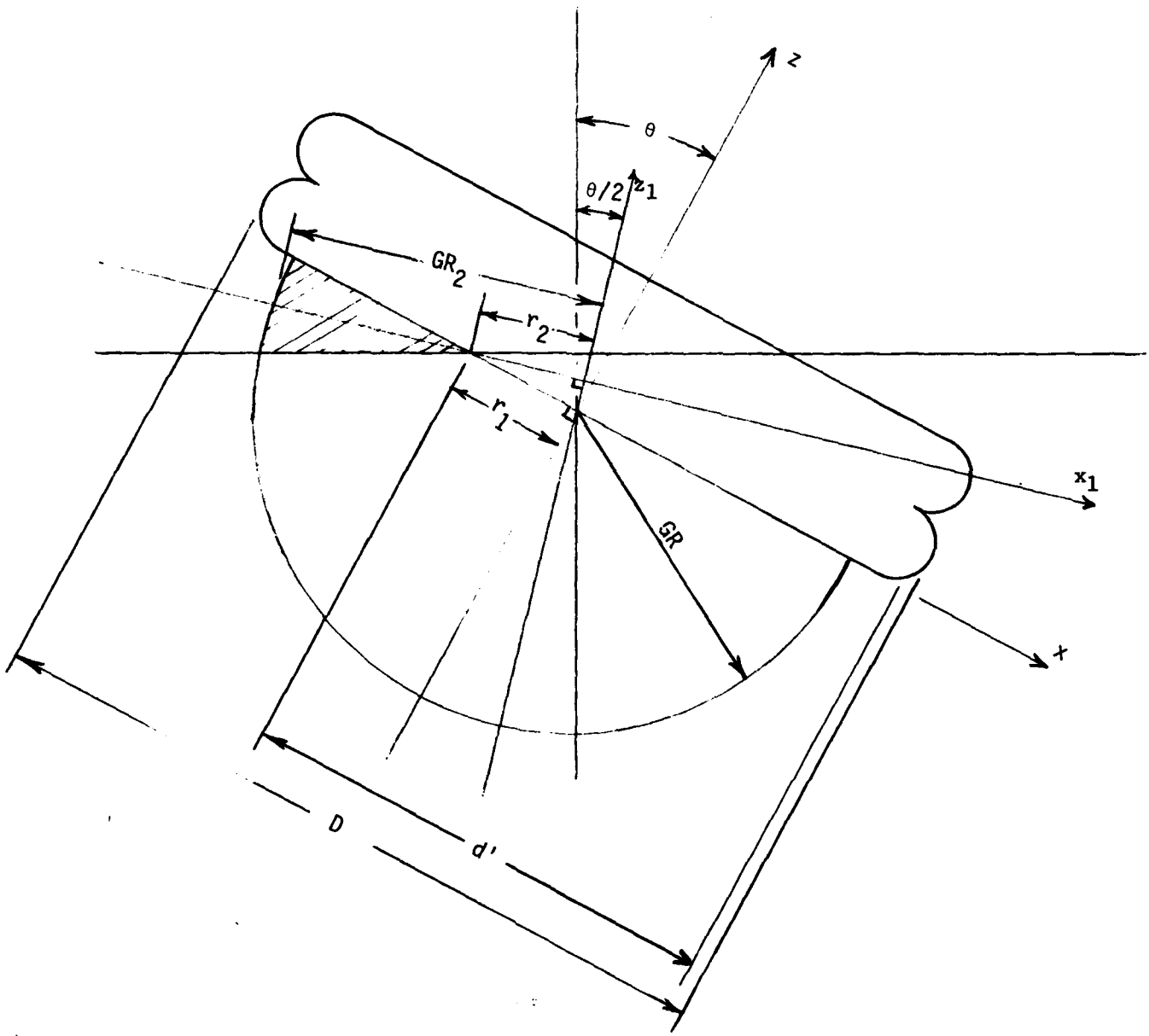

FIGURE 4-6

GEOMETRICAL DEFINITIONS FOR DETERMINING
BALLAST WEIGHT AND CENTER OF GRAVITY OF HEMISPHERICAL BALLAST BAG

$$GR_2 = \sqrt{GR^2 - r_1^2 \sin^2 \frac{\theta}{2}}$$

Then the volume of the segmental wedge can be obtained by integration as follows:

$$Vol = 4 \tan\left(\frac{\theta}{2}\right) \int_{-GR_2}^{r_2} (r_2 - x_1) \sqrt{GR_2^2 - x_1^2}\, dx_1$$

which becomes:

$$Vol = 4 \tan\left(\frac{\theta}{2}\right) \left\{ \frac{r_2}{2} \left[r_2 \sqrt{GR_2^2 - r_2^2} + GR_2^2 \left(\sin^{-1} \frac{r_2}{GR_2} + \frac{\pi}{2}\right)\right] + \frac{1}{3} \sqrt{(GR_2^2 - r_2^2)^3} \right\}$$

$$BA = w \cdot VOL$$

Similarly, the moment of volume about the center of the mean circular segment can can be obtained by integration as follows:

$$MOM = 4 \tan\left(\frac{\theta}{2}\right) \int_{-GR_2}^{r_2} x_1 (r_2 - x_1) \sqrt{GR_2^2 - x_1^2}\, dx_1$$

which becomes:

$$MOM = -\tan\left(\frac{\theta}{2}\right) \left\{ \frac{r^2}{3} \sqrt{GR_2^2 - r_2^2)^3} + \frac{GR_2^2}{2} \left[r_2 \sqrt{GR_2^2 - r_2^2} + GR_2^2 \left(\sin^{-1} \frac{r_2}{GR_2} + \frac{\pi}{2}\right)\right] \right\}$$

By geometry, the moment arm of the ballast weight, BA, about the center of buoyancy is:

$$ba = \left\{ \bar{x} + \left(r_2 - \frac{MOM}{VOL}\right) \cos\frac{\theta}{2} - r_1 + \left[\bar{z} + \left(r_2 - \frac{MOM}{VOL}\right) \sin\frac{\theta}{2} \right] \tan\theta \right\} \cos\theta$$

4.3.4 Toroidal Ballast Bag

When a liferaft with a toroidal ballast bag pitches, a cylindrical wedge of ballast water rises above the water surface. If the raft pitches to a sufficient angle that the bottom of the ballast bag is above the water surface, then the volume of the wedge will be truncated by the bottom and, in general, the volume will also be reduced by the volume of the void wedge inside the toroid. For the Quasi-Static Model, the overall diameter of the toroid is assumed to be equal to the outside diameter of the liferaft, D. The volume and moment of volume of the wedge of ballast water depends upon the outside radius, R, the inside radius, IR, the depth of the ballast bag, k, and the pitch angle, θ. The geometry of the toroidal ballast bag is shown in Figure 4-7.

The procedure for calculating the volume and moment of the ballast water is to first calculate the volume and moment of a cylindrical wedge of an assumed cylindrical ballast bag of infinite depth and no internal void (IR = 0). This volume would be the total of Section (A), (B), and (C) shown in Figure 4-7. Then, the volumes and moments which are not properly a part of the toroidal ballast bag i.e. Sections (B) and (C), are calculated and deducted from the gross volume and moment of the toroidal ballast bag. That is:

$$V_{(A)} = V_{(A) + (B) + (C)} - V_{(B)} - V_{(C)}$$

and

$$M_{(A)} + M_{(A) + (B) + (C)} - M_{(B)} - M_{(C)}$$

where V and M are volume and moment, respectively, and the subscripts refer to the sections of the ballast bag. The individual elements are calculated as follows:

$$V_{(A) + (B) + (C)} = 2 \int_{o}^{2R-d'} h\, y\, dx$$

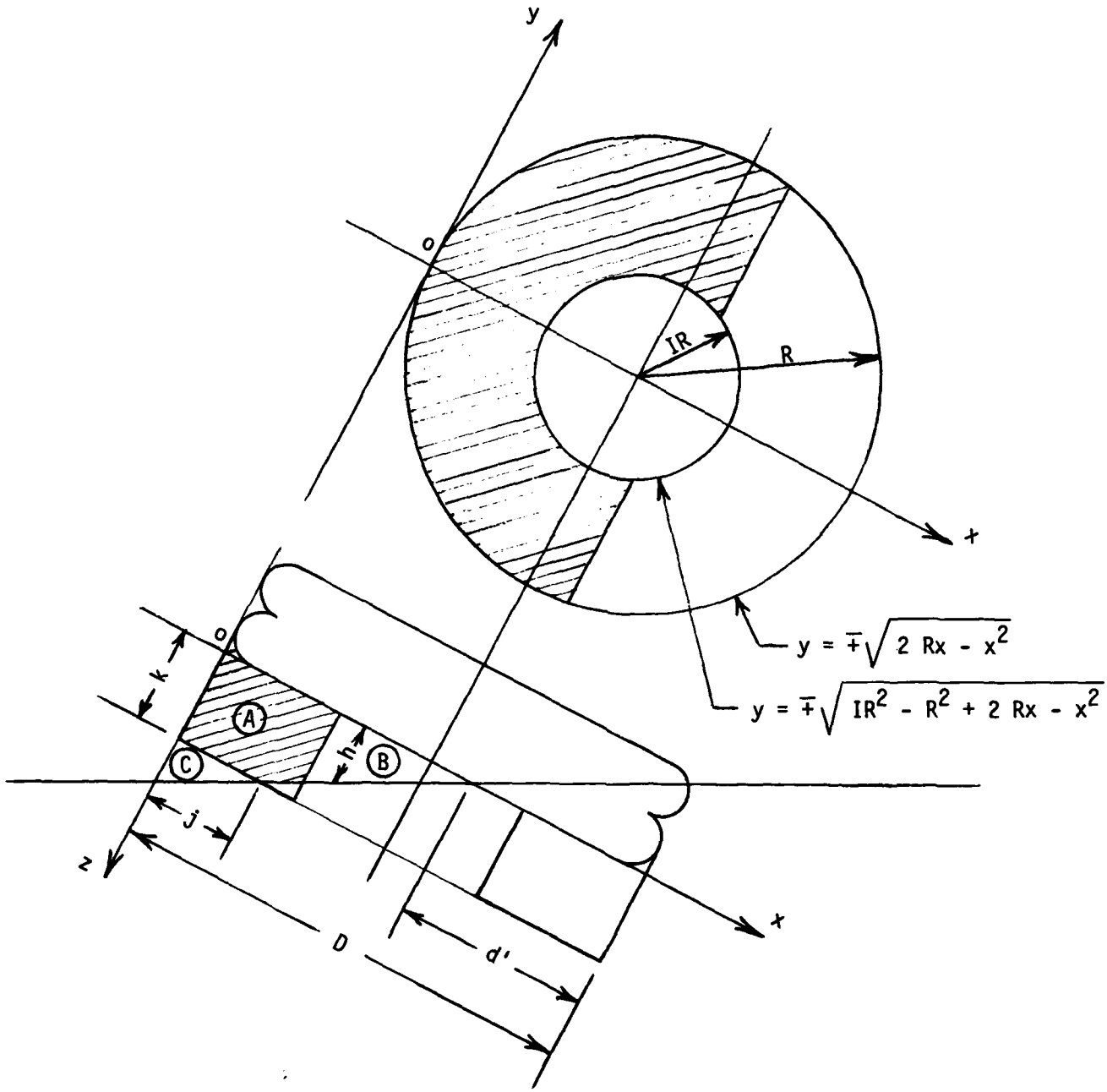

FIGURE 4-7

GEOMETRICAL DEFINITIONS FOR DETERMINING

BALLAST WEIGHT AND CENTER OF GRAVITY OF

TOROIDAL BALLAST BAG

Since

$$h = (2R - d' - x) \tan \theta$$

and

$$y = \mp \sqrt{2Rx - x^2}$$

then

$$V_{(A) + (B) + (C)} = 2 \tan \theta \int_0^{2R-d'} (2R - d' - x) \sqrt{2Rx - x^2}\, dx$$

which becomes

$$V_{(A) + (B) + (C)} = \tan \theta \left\{ (R-d')^2 \sqrt{2Rd' - d'^2} + R^2 (R - d') \left[\sin^{-1} \left(\frac{R - d'}{R} \right) + \frac{\pi}{2} \right] + \frac{2}{3} (2Rd' - d'^2)^{3/2} \right\}$$

Similarly, the moment of the ballast volume about the z axis, $M_{z(A) + (B) + (C)}$ is obtained from the integration:

$$M_{z(A) + (B) + (C)} = 2 \int_0^{2R-d'} x\, h\, y\, dx$$

thus

$$M_{z(A) + (B) + (C)} = 2 \tan \theta \int_0^{2R-d'} x\, (2R-d'-x) \sqrt{2Rx-x^2}\, dx$$

which becomes

$$M_{z(A)+(B)+(C)} = \tan\theta\left\{\left(\frac{3R}{4} - d'\right)\left[\left(R^2 - Rd'\right)\sqrt{2Rd' - d'^2}\right.\right.$$

$$\left.\left. + R^3\left(\sin^{-1}\frac{R-d'}{R} + \frac{\pi}{2}\right)\right] + \left(\frac{R}{2} + \frac{d'}{6}\right)\left(2Rd' - d'^2\right)^{3/2}\right\}$$

And the moment of the ballast volume below the x axis, $M_{x(A)+(B)+(C)}$, is obtained from a similar integration:

$$M_{x(A)+(B)+(C)} = 2\int_0^{2R-d'} \frac{h^2}{2}\, y\, dx$$

thus

$$M_{x(A)+(B)+(C)} = \tan^2\theta \int_0^{2R-d'} (2R - d' - x)^2\sqrt{2Rx - x^2}\, dx$$

which becomes

$$M_{x(A)+(B)+(C)} = \tan^2\theta\left\{\left(\frac{5R^2}{8} - Rd' + \frac{d'^2}{2}\right)\left[(R-d')\sqrt{2Rd'-d'^2}\right.\right.$$

$$\left.\left. + R^2\left(\sin^{-1}\frac{R-d'}{R} + \frac{\pi}{2}\right)\right] + \frac{5(R-d')}{12}\left(2Rd'-d'^2\right)^{3/2}\right\}$$

The volume and moment of the (B) section (i.e. the interior void of the toroid) is calculated according to one of three sets of formulas depending upon the intersection of the waterline with the flat bottom of the raft (i.e. the value of d'). The first alternative occurs when the flat bottom of the raft within the inside of the toroid is entirely below the water surface (i.e., d' > R + IR). In this case (B) does not exist and $V_{(B)} = 0$, $Mx_{(B)} = 0$, and $Mz_{(B)} = 0$.

The second alternative is when the flat bottom of the raft intersects the water surface within the inside of the toroid, i.e.

$$R + IR > d' > R - IR$$

In this case (B) is a wedge of a cylinder. The volume, $V_{(B)}$, is obtained from the integration

$$V_{(B)} = 2 \int_{R-IR}^{2R-d'} h\, y\, dx$$

Since

$$h = (2R - d' - x) \tan \theta$$

and

$$y = \pm\sqrt{IR^2 - R^2 + 2xR - x^2}$$

then

$$V_{(B)} = 2 \tan \theta \int_{R-IR}^{2R-d'} (2R - d' - x)\sqrt{IR^2 - R^2 + 2xr - x^2}\, dx$$

which becomes

$$V_{(B)} = \tan \theta \left\{(R - d')^2\sqrt{IR^2 - R^2 + 2Rd' - d'^2}\right.$$
$$+ (R - d')\, IR^2 \left[\sin^{-1} \left(\frac{R-d}{IR}\right) + \frac{\pi}{2}\right]$$
$$\left. + 2/3\, (IR^2 - R^2 + 2Rd' - d'^2)^{3/2}\right\}$$

The moment of volume of Section (B) about the z axis, $M_{z(B)}$ is obtained from the integration:

$$M_{z(B)} = 2 \int_{R-IR}^{2R-d'} x\ h\ y\ dx$$

thus

$$M_{z(B)} = 2 \tan \theta \int_{R-IR}^{2R-d'} x(2R - d' - x)\sqrt{IR^2 - R^2 - 2xR - x^2}\ dx$$

which becomes

$$M_{z(B)} = \tan \theta \left\{ \left(\frac{3R + d'}{6}\right) (IR^2 - R^2 - 2Rd' - d'^2)^{3/2} + (R^2 - Rd' - \frac{IR^2}{4}) \left[(R - d') \sqrt{IR^2 - R^2 + 2Rd' - d'^2} + IR^2 \left(\sin^{-1} \frac{R-d'}{IR} + \frac{\pi}{2}\right)\right]\right\}$$

The moment of volume of Section (B) about the x axis, $M_{x(B)}$, is obtained from the integration

$$M_{x(B)} = 2 \int_{R-IR}^{2R-d'} \frac{h}{2}\ h\ y\ dx$$

thus

$$M_{x(B)} = \tan^2 \theta \int_{R-IR}^{2R-d'} (2R - d' - x)^2 \sqrt{IR^2 - R^2 + 2xR - x^2}\ dx$$

which becomes

$$M_{x(B)} = \tan^2\theta \left\{ \left(R^2 - 2Rd' + d'^2 + \frac{IR^2}{4}\right) \left[\frac{IR^2}{2} \left(\sin^{-1} \frac{R-d'}{IR} + \frac{\pi}{2}\right) \right.\right.$$

$$\left. + \frac{R-d'}{2} \sqrt{IR^2 - R^2 + 2Rd' - d'^2} \right]$$

$$\left. + \frac{5(R - d')}{12} \left(IR^2 - R^2 + 2Rd' - d'^2\right)^{3/2} \right\}$$

The third alternative in connection with Section (B) occurs when the flat bottom of the raft within the toroid is entirely above the water surface, i.e. $d' < R - IR$. In this case the Section (B) is a full cylinder with a sloped bottom. The volume $V_{(B)}$ is obtained from the integration

$$V_{(B)} = \pi\, IR^2\, (R - IR - d')\, \tan\theta$$

$$+ 2 \int_{R-IR}^{R+IR} h\, y\, dx$$

Since

$$h = (R + IR - x) \tan\theta$$

and

$$y = \mp \sqrt{IR^2 - R^2 + 2Rx - x^2}$$

then

$$V_{(B)} = \pi\, IR^2\, (R - IR - d')\, \tan\theta$$

$$+ 2\, \tan\theta \int_{R-IR}^{R+IR} (R + IR - x) \sqrt{IR^2 - R^2 + 2Rx - x^2}\; dx$$

which becomes

$$V_{(B)} = \pi\, IR^2\, (R - d')\, \tan\theta$$

Similarly, the moment of volume of Section (B) about the z axis, $M_{z(B)}$ is obtained from the integration

$$M_{z(B)} = R\pi\, IR^2\, (R - IR - d')\, \tan\theta$$

$$+ 2 \int_{R-IR}^{R+IR} x\, h\, y\, dx$$

thus,

$$M_{z(B)} = R\pi\, IR^2\, (R - IR - d')\, \tan\theta$$

$$+ 2\, \tan\theta \int_{R-IR}^{R+IR} x(R + IR - x) \sqrt{IR^2 - R^2 + 2Rx - x^2}\; dx$$

which becomes

$$M_{z(B)} = \pi\, IR^2\, \tan\theta\, (R^2 - Rd' - \frac{IR^2}{4})$$

The moment of volume of Section (B) about the x axis, $M_{x(B)}$, is obtained from a similar integration

$$M_{x(B)} = \frac{\pi\, IR^2}{2}\ (R - IR - d')^2\ \tan^2\theta$$

$$+ \pi\, IR^3\ (R - IR - d')\ \tan^2\theta$$

$$+ 2\int_{R-IR}^{R+IR} \frac{h}{2}\, h\, y\, dx$$

thus

$$M_{x(B)} = \pi\, IR^2\ \tan^2\theta\left[\frac{(R - IR - d')^2}{2} + IR\ (R - IR - d')\right]$$

$$+ \tan^2\theta \int_{R-IR}^{R+IR} (R + IR - x)^2 \sqrt{IR^2 - R^2 - 2Rx - x^2}\ dx$$

which becomes

$$M_{x(B)} = \pi\, IR^2\ \tan^2\theta\ \left(\frac{R^2}{2} - Rd' + \frac{IR^2}{8} + \frac{d'^2}{2}\right)$$

The circular wedge of volume between the bottom of the toroidal ballast bag and the surface of the water, designated Section (C) in Figure 4-7 depends upon the intersection of the bottom of the toroidal ballast bag and the water surface. The distance of this point of intersection from the center of the coordinate system is designated j and is calculated from

$$j = D - d' - \frac{k}{\tan\theta}$$

If $j \leq 0$, then the bottom of the toroidal ballast bag is fully immersed and the volume (and moments) of (C), $V_{(C)}$ (and $Mx_{(C)}$ and $Mz_{(C)}$)is zero. Otherwise, $V_{(C)}$ is obtained from the integration

$$V_{(C)} = 2 \int_0^j h\, y\, dx$$

Since

$$h = (j - x) \tan \theta$$

and

$$y = \pm\sqrt{2Rx - x^2}$$

then

$$V_{(C)} = 2 \tan \theta \int_0^j (j - x) \sqrt{2Rx - x^2}\ dx$$

which becomes

$$V_{(C)} = \tan \theta \left\{ (j - r)^2 \sqrt{2Rj - j^2} + R^2 (j - R) \left[\sin^{-1} \frac{j-R}{R} + \frac{\pi}{2}\right] + \frac{2}{3} (2Rj - j^2)^{3/2} \right\}$$

Similarly the moment of volume of Section (C) about the z axis is obtained from the integration

$$M_{z(C)} = 2 \int_0^j x\, h\, y\, dx$$

thus

$$M_{z(C)} = 2 \tan \theta \int_0^j x(j - x) \sqrt{2Rx - x)^2}\ dx$$

which becomes

$$M_{z(C)} = \tan \theta \left\{(j - \frac{5R}{4}) \left[R(j - R) \sqrt{2Rj - j^2}\right.\right.$$

$$\left. - \frac{2}{3} (2Rj - j^2)^{3/2} + R^3 (\sin^{-1} \frac{j - R}{R} + \frac{\pi}{2})\right]$$

$$\left. + \frac{j}{2} (2Rj - j^2)^{3/2}\right\}$$

The moment of volume of Section (C) about the x axis, $M_{x(C)}$ is obtained from the integration

$$M_{x(C)} = k V_{(C)} + 2 \int_0^j \frac{h^2}{2} y\ dx$$

thus

$$M_{x(C)} = k V_{(C)} + \tan^2 \theta \int_0^j (j - x)^2 \sqrt{2Rx - x^2}\ dx$$

which becomes

$$M_{x(C)} = k V_{(C)} + \tan^2 \theta \left\{(j^2 - 2jR + \frac{5R^2}{4})\right.$$

$$\left[(j - R) \sqrt{2jR - j'^2} + R^2 (\sin^{-1} \frac{j - R}{R} + \frac{\pi}{2})\right]$$

$$\left. + \frac{5 (j - R)}{12} (2jR - j'^2)^{3/2}\right\}$$

The net moment arms of the toroidal ballast bag volume Section (A) about the x axis, x b a, and the z axis, z b a, are obtained as follows

$$\overline{xba} = \frac{M_{z(A)+(B)+(C)} - M_{z(B)} - M_{z(C)}}{V_{(A)+(B)+(C)} - V_{(B)} - V_{(C)}}$$

and

$$\overline{zba} = \frac{M_{x(A)+(B)+(C)} - M_{x(B)} - M_{x(C)}}{V_{(A)+(B)+(C)} - V_{(B)} - V_{(C)}}$$

Then by geometry the moment arm of the ballast weight, BA of the toroidal ballast bag about the center of buoyancy, b a, is

$$ba = \left[\bar{x} + \frac{D}{2} - \overline{xba} + (\bar{z} + \overline{zba}) \tan\theta\right]\cos\theta$$

5.0 WIND TUNNEL TESTS

It was already appreciated before this study commenced that liferaft capsizing is often caused by wind forces acting on the flat bottom surface of the raft when it becomes exposed. The quasi-static inflatable liferaft stability model was developed to fully account for the influence of the wind force on the capsizing moment. The wind lift, drag, and moment are applied in the model as functions of the pitch angle and the length of bottom exposed. Each are calculated from their coefficients.

In similar situations the aerodynamic coefficients are obtained from available aerodynamics data or from wind tunnel model tests. No appropriate aerodynamic coefficient data could be found therefore it was necessary to perform wind tunnel tests to obtain the coefficients for the four inflatable liferaft configurations.

5.1 Test Set Up

The ten foot low speed wind tunnel at the California Institute of Technology in Pasadena was selected to perform the test. The standard procedure for testing a model of an object in close proximity to the ground (or the water surface in the case of a liferaft) is to place a groundboard near the center of the tunnel. The model is suspended above the groundboard so that it does not touch it (to eliminate spurious frictional forces when the wind load is applied) but so close that air cannot flow through the gap where the model would normally be in contact with the surface. This type of test arrangement was impractical for the inflatable liferaft test because the immersed portion of the raft model would have to be eliminated. Since each test condition (pitch angle, length of bottom exposure, and ballast bag configuration) has a unique intersection with the water surface, there would have to be a separate model modification for each test condition.

In lieu of this, the tests were made with the complete model suspended within a circular cutout in the groundboard. An enclosure was fitted below the groundboard cutout to shield the simulated below-water portion of the liferaft model from the wind stream beneath the groundboard. Flush insert pieces enclose the spaces left open in the groundboard cutout due to the orientation of the model.

A gap is maintained between the model and the groundboard to eliminate spurious loads that would occur if the model touched the groundboard during testing. The gap was sealed all around with soft close-celled foam rubber to prevent air flow within the enclosure beneath the groundboard. The model is suspended on a single strut from the balances located above the wind tunnel test section. A diagram of the test set up is shown in Figure 5-1. The arrangement of the groundboard in the tunnel test section with the model mounted in two typical positions is shown in Figure 5-2 and 5-3.

Blockage beneath the groundboard due to the enclosure caused a flow up and around the leading edge of the groundboard disturbing the boundary layer on the surface of the groundboard. This was controlled by a turning vane installed along the leading edge of the groundboard as shown in Figure 5-4.

Note: It was originally intended that the tank which enclosed the model beneath the groundboard would be filled with water to the level of the top of the groundboard to complete the enclosure of the surface around the model. Sheet metal extensions of the groundboard to within a close proximity of the sides of the model were to mitigate the effect of the wind on the surface of the water. That approach was abandoned in favor of the procedure described above when it proved impossible to prevent the water from being blown out no matter how close the gap between the sheet metal and the model.

5.2 Model

As an economy measure the liferaft model for the wind tunnel tests was also intended to be used for the wave tank tests. The scale ratio of the model was therefore based upon considerations for both tests. The basic considerations were that the model be large enough to minimize scale effects, large enough that the Reynolds number be well above the transition flow regime for wind tunnel tests, and small enough that the available wind in the wave tank was sufficient to capsize the model.

Preliminary wind force and moment coefficients from a British wind tunnel test(ref. 6) of a full size inflatable liferaft were applied in a preliminary version of the quasi-static stability model to show that a three foot diameter model would be unstable at 30 degrees in the light condition with the 19 knot wind available at

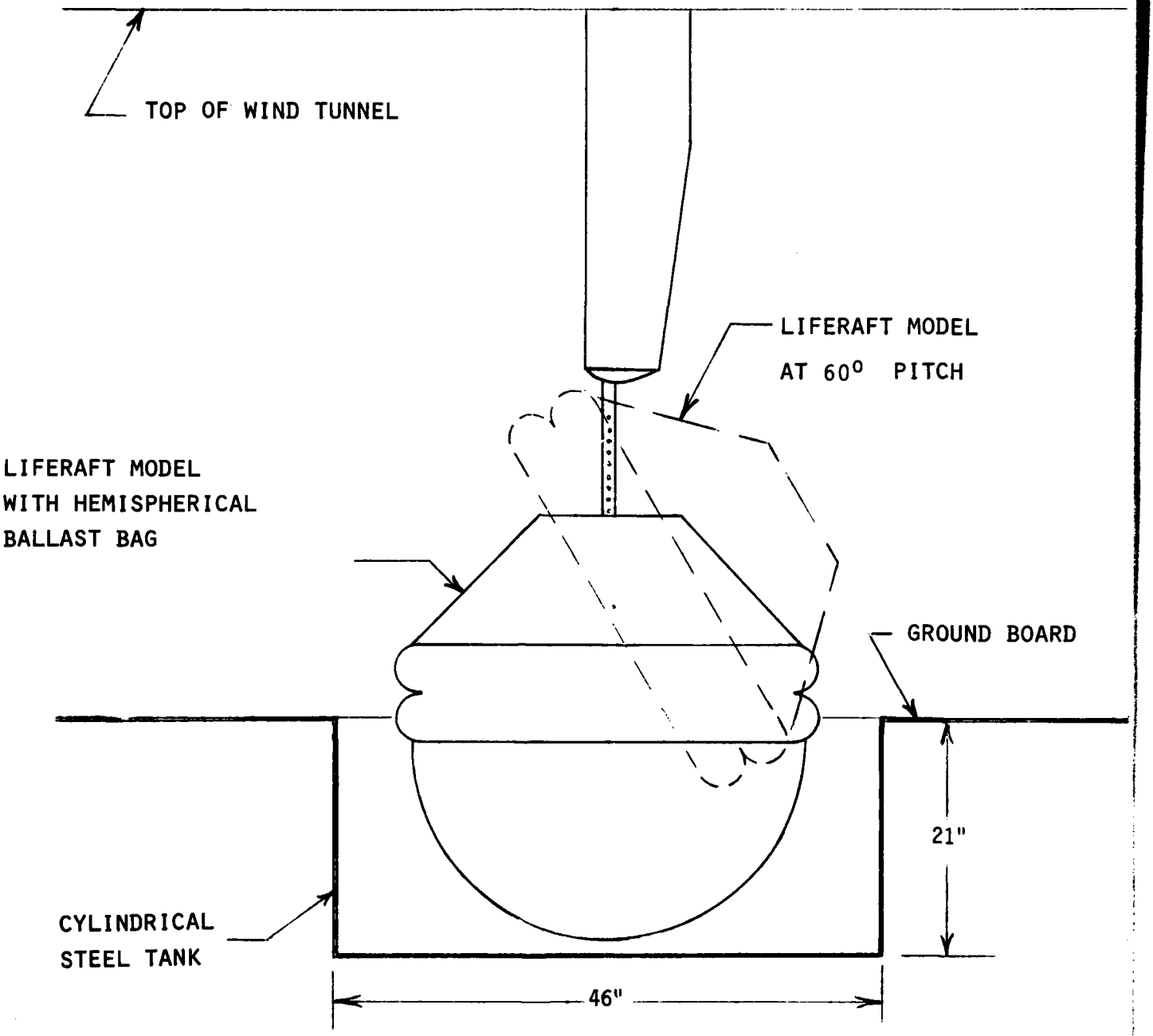

FIGURE 5-1

DIAGRAM OF WIND TUNNEL TEST SETUP

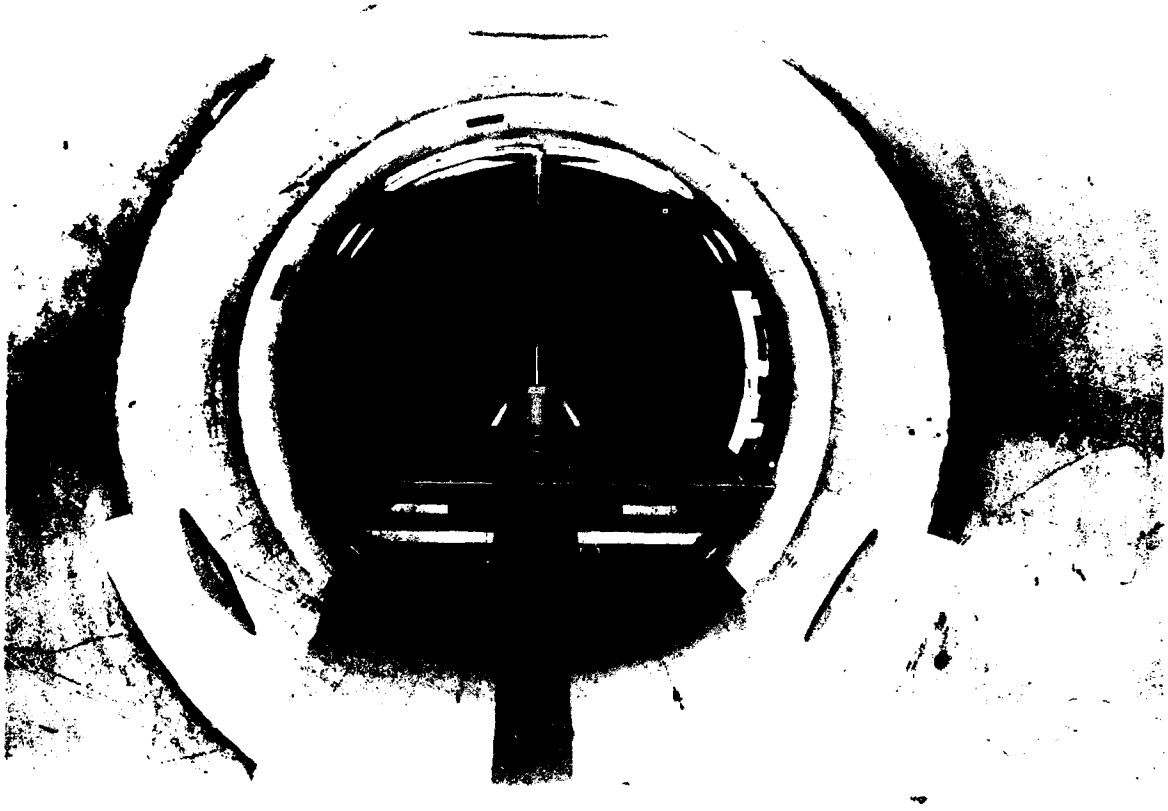

FIGURE 5-2

VIEW OF WIND TUNNEL TEST SECTION FROM UPWIND

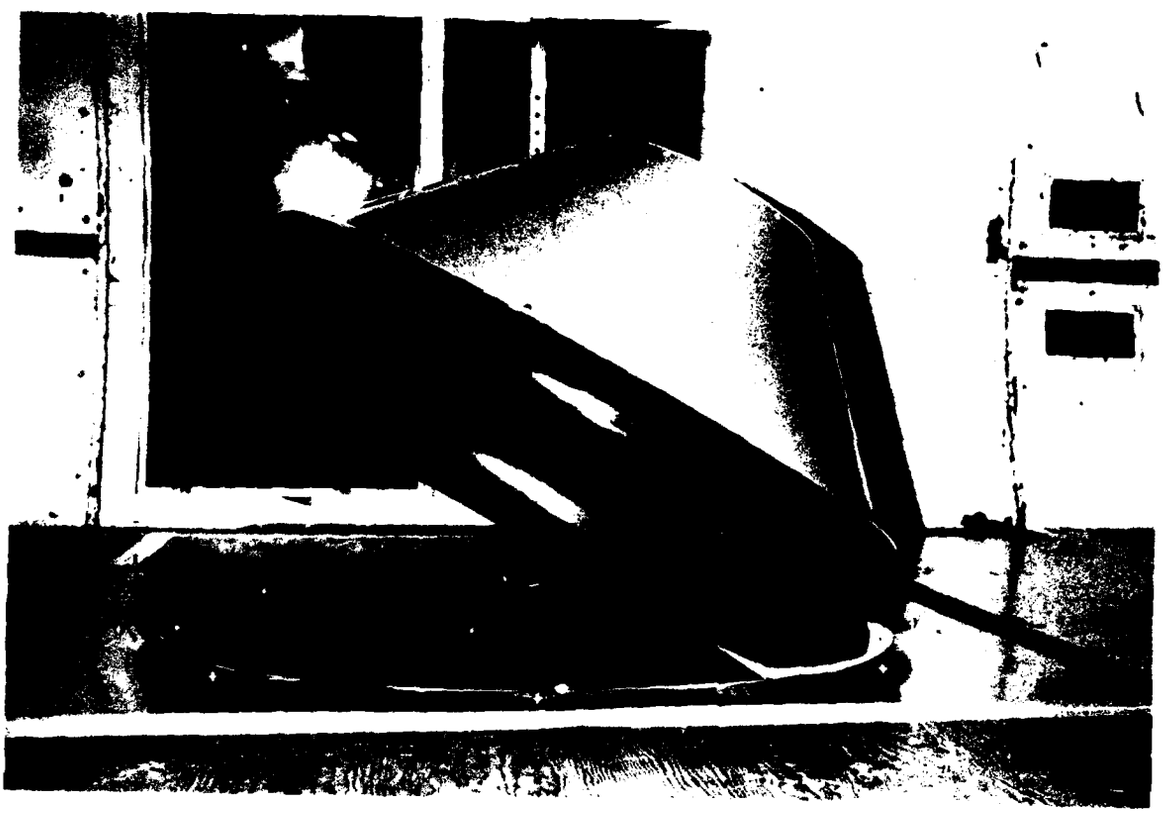

FIGURE 5-3

VIEW OF LIFERAFT MODEL IN PLACE OVER GROUNDBOARD IN WIND TUNNEL

FIGURE 5-4

TURNING VANE AT LEADING EDGE OF GROUNDBOARD

the wave tank. This size model would have a sufficiently high Reynolds number in the wind tunnel and also was about the largest size model that would be accomodated in the test section.

The model is intended to be representative of inflatable liferafts in general rather than any specific manufacturer's design. The liferaft is composed of two toroidal tubes, one on top of the other. The proportions of the raft are based on the U.S. Coast Guard capacity requirements, Section 160.051-4(i) of Reference 5. There must be 4 square feet of clear inside area and 3.4 cubic feet of volume in the inflated tubes per person. The overall diameter, D, and the tube cross section diameter, t, can then be related to the capacity, P, by the relations:

$$4\,P = \pi\,\frac{(D-2t)^2}{4}$$

and

$$3.4\,P = 2\pi^2\,(D - t)\,\left(\frac{t^2}{4}\right)$$

Solution of these equations for a six man capacity raft indicates an 86 inch overall diameter and 10 inch tube diameter. The three foot diameter model would therefore have a scale ratio of 42 percent of a six man liferaft. The same model would also be a 20 percent scale model of a 25 man raft although the tube diameter would be about 30 percent greater than necessary.

The model is fitted with a canopy. It was recognized that the aerodynamic loads would be somewhat affected by whether a canopy is or is not erected, by the orientation and configuration of an opening whether the opening is closed or not, and by the flexibility of the canopy. It was judged that these are secondary factors in stability. Any effort to include testing variations of the canopy configuration would detract from the primary objective of defining the wind force and pitch moment coefficients as functions of pitch angle and bottom exposure. Therefore, a rigid canopy with no opening was used throughout the tests. In any case, the effect of canopy openings and orientation has been thoroughly explored in the British full scale liferaft wind tunnel test referred to above.

Similarly, it was recognized that the flexibility of an inflatable liferaft influences the aerodynamic forces due to both surface flexibility (which influences the friction forces) and gross geometrical distortions. Since the degree of flexibility would be expected to vary considerably depending upon the construction of the raft and the inflation pressure, modelling the flexibility could become very involved. In any event, interpretation of the results of wind tunnel tests of a flexible model would have to include consideration of the relative contributions of flexibility and geometrical variations. This would be difficult, at best, and probably impossible with the current state of the art. As a result of these considerations, the model was designed to be rigid so that the test results would apply to a well defined geometrical shape.

The model was build of foam on a plywood base and fiberglassed on the exterior. The construction details of the model are shown in Figure 5-5. Construction details for the ballast pockets, toroidal ballast bag, and hemispherical ballast bag modifications to the model are shown in Figure 5-6, 5-7, and 5-8 respectively. It should be noted that neutral buoyancy (to simulate the weight of the free-flooding ballast water) in the ballast bags, which is necessary for the wave tank tests, was not necessary for the wind tunnel tests which depend only upon geometry. Therefore, the uniformly spaced lead weights imbedded in the foam to achieve the neutral buoyancy condition were removed for the wind tunnel tests. (The hemispherical ballast bag is a fiberglass hemisphere designed to be filled with water in the wave tank tests. It was empty in the wind tunnel tests.) The alternative methods used to ballast the model were selected on the basis of economy of model construction.

The model was held from the strut arm by a fixture, shown in Figure 5-9, which permits the model to be set at pitch angles in 10 degree increments from zero to 60 degrees and at vertical displacements with respect to the ground board in 1/8 inch increments.

5.3 Testing

With the model set at zero degrees pitch angle, force and moment measurements were taken with the wind speed varied to produce dynamic pressures from 3 to 14 pounds per square feet. Absence of transition flow effects and repeatability of data was demonstrated at 12 pounds per square feet and all subsequent tests were

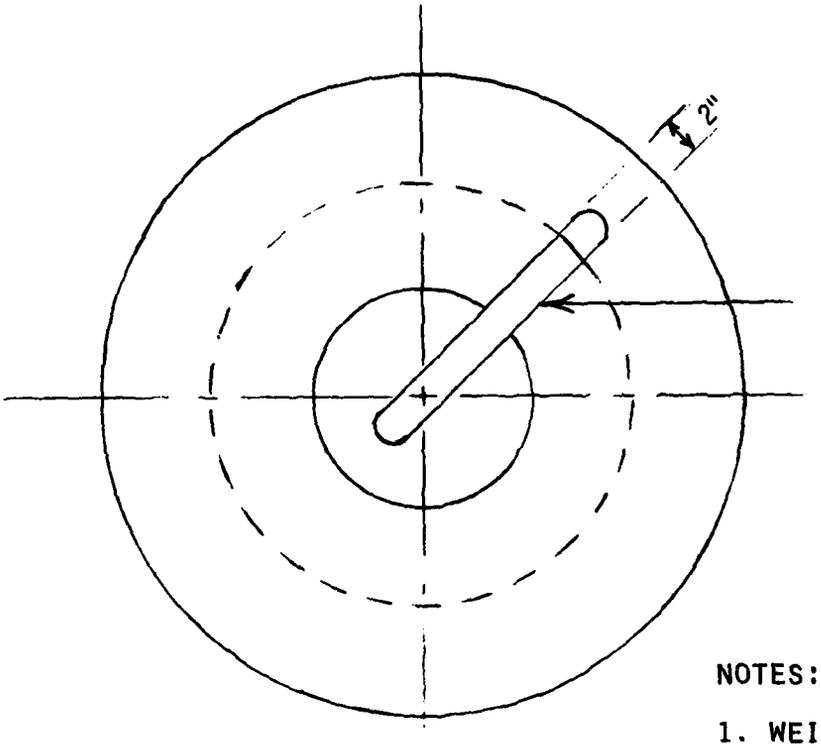

NOTES:

1. WEIGHT = 20 LBS.
2. EXTERIOR FIBERGLASSED

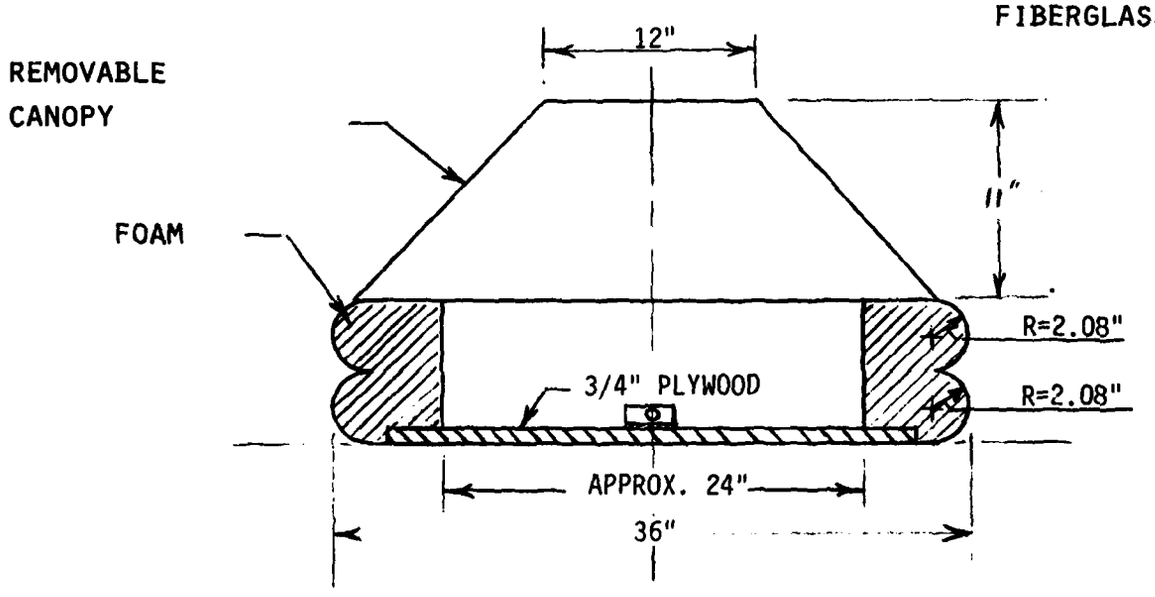

FIGURE 5-5

CONSTRUCTION DETAILS OF

6 MAN INFLATABLE LIFERAFT MODEL

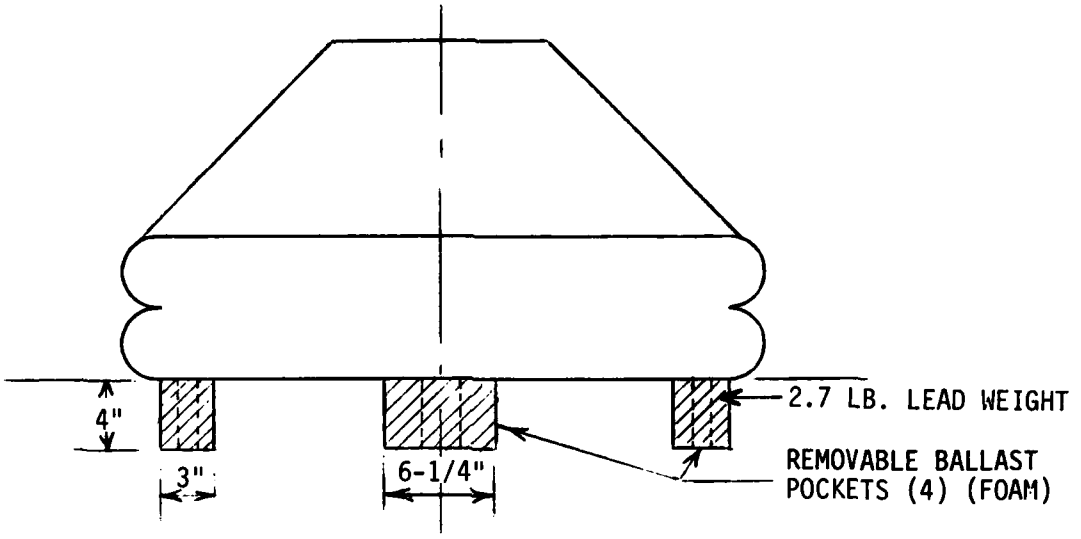

FIGURE 5-6

CONSTRUCTION DETAILS OF

BALLAST POCKETS

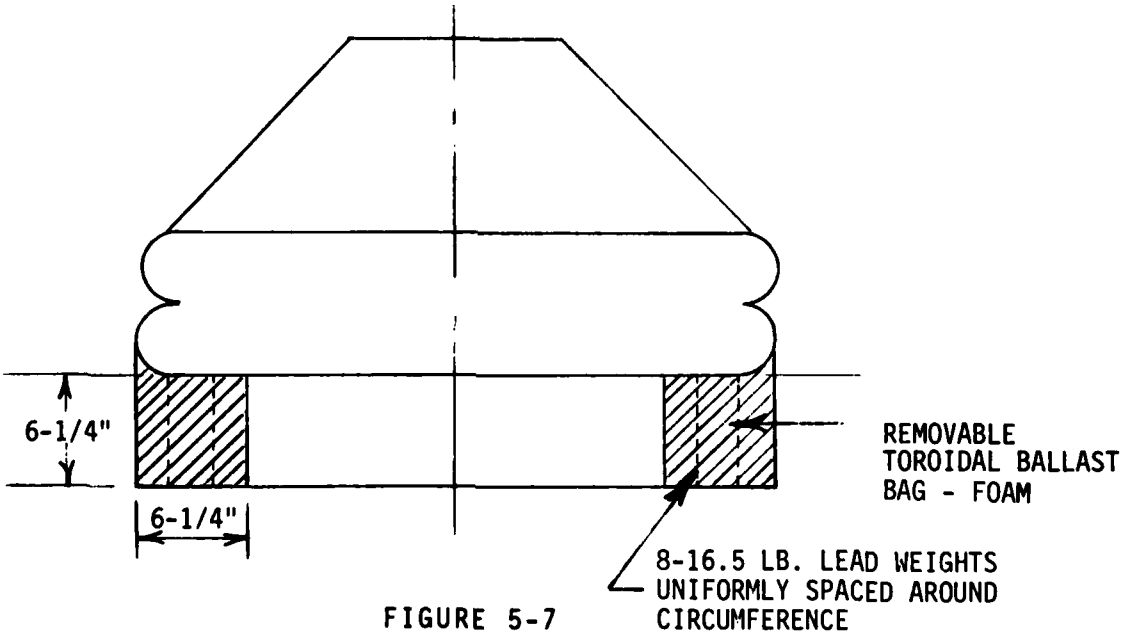

FIGURE 5-7

CONSTRUCTION DETAILS OF

TOROIDAL BALLAST BAG

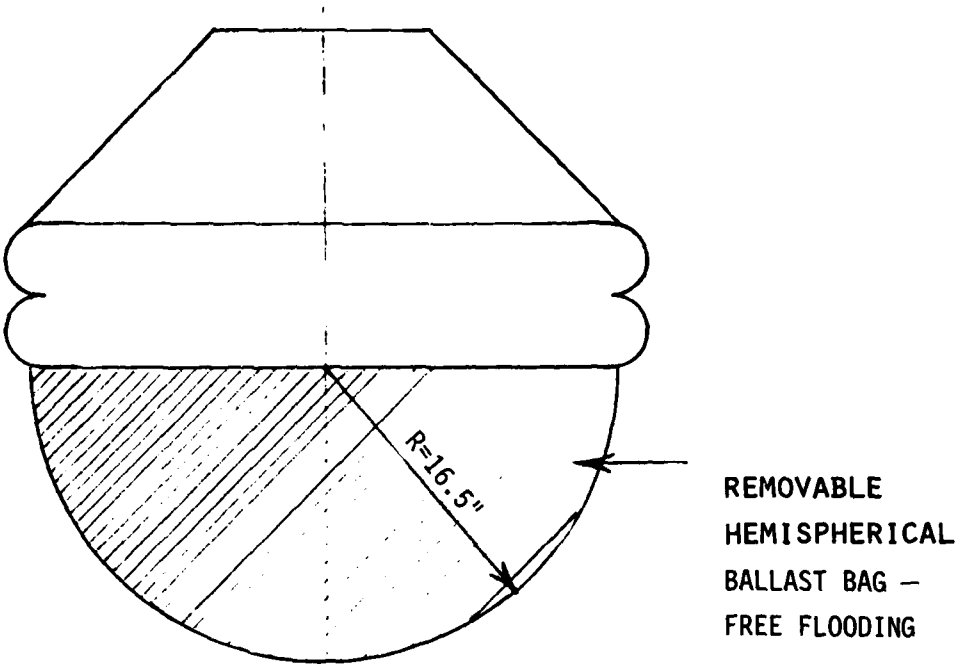

FIGURE 5-8

CONSTRUCTION DETAILS OF

HEMISPHERICAL BALLAST BAG

FIGURE 5-9

DETAILS OF MODEL SUPPORT FIXTURE

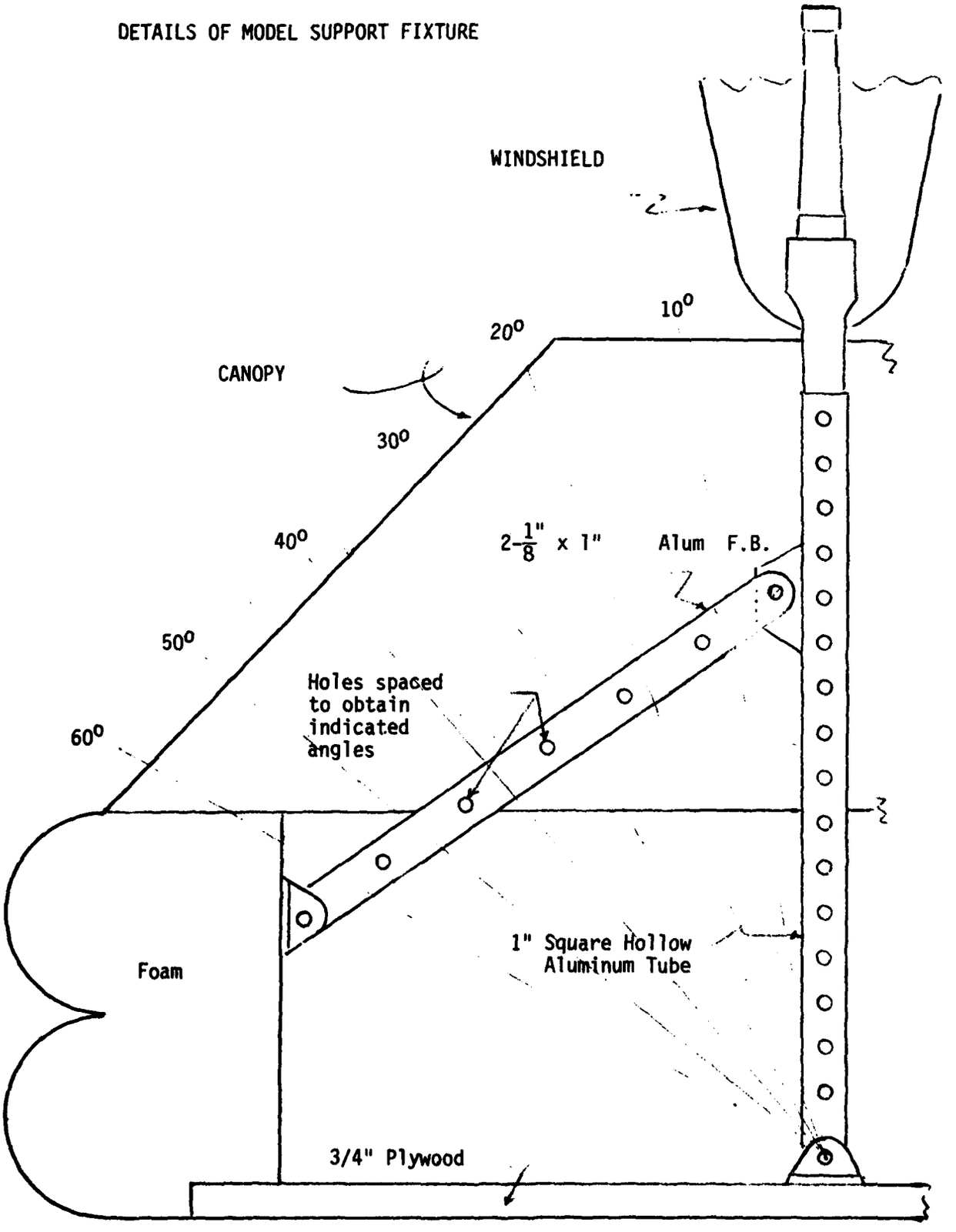

conducted at that speed.

Lift, drag, and the moment about the centroid were measured with respect to the coordinate system shown in Figure 4-4. The data were non-dimensionalized and presented as the coefficients C_D, C_L, and C_M according to the definitions given in Section 4.2. Measurements were taken at every 10 degrees of pitch from zero to 60 degrees and for five values of bottom immersion from zero to 100 percent of the diameter. Exceptions to this are at high pitch angles where the strut arrangement would not permit very small lengths of bottom immersion and where combinations of pitch angle and large lengths of bottom immersion would cause the raft to be in an unrealistic swamped condition.

The flat bottom configuration was tested through the complete range of angles and bottom immersions. Some representative test conditions are shown in Figure 5-10 and 5-11.

The ballast pocket configuration was tested in three representative conditions at which point it was observed that there was no significant difference between the flat bottom configuration and no further tests were made. The condition at ten degrees pitch angle and zero length of bottom immersion is shown in Figure 5-12.

The hemispherical ballast bag configuration was tested at five combinations of pitch angle and displacement. Conditions with small values of d' (which would be the length of immersed bottom for the flat bottom configuration) were considered unrealistic because there would be very little buoyancy to support the heavy weights of ballast that would be lifted out of the water in those conditions. Similarly large pitch angles at large lengths of bottom immersion are unrealistic and were not tested because the low side of the raft would be swamped. Figure 5-13 shows the model with the hemispherical ballast bag suspended above the ground board cutout. Figure 5-14 shows the model with the hemispherical ballast bag at 30 degrees and d' at 47 percent of D. Figure 5-15 shows the model at 20 degrees and d' at 47 percent of D.

The model with the toroidal ballast bag was tested in three conditions. Two tests at 20 degrees where the bottom of the ballast bag did not emerge from the water confirmed that the aerodynamic coefficients are not appreciably different from

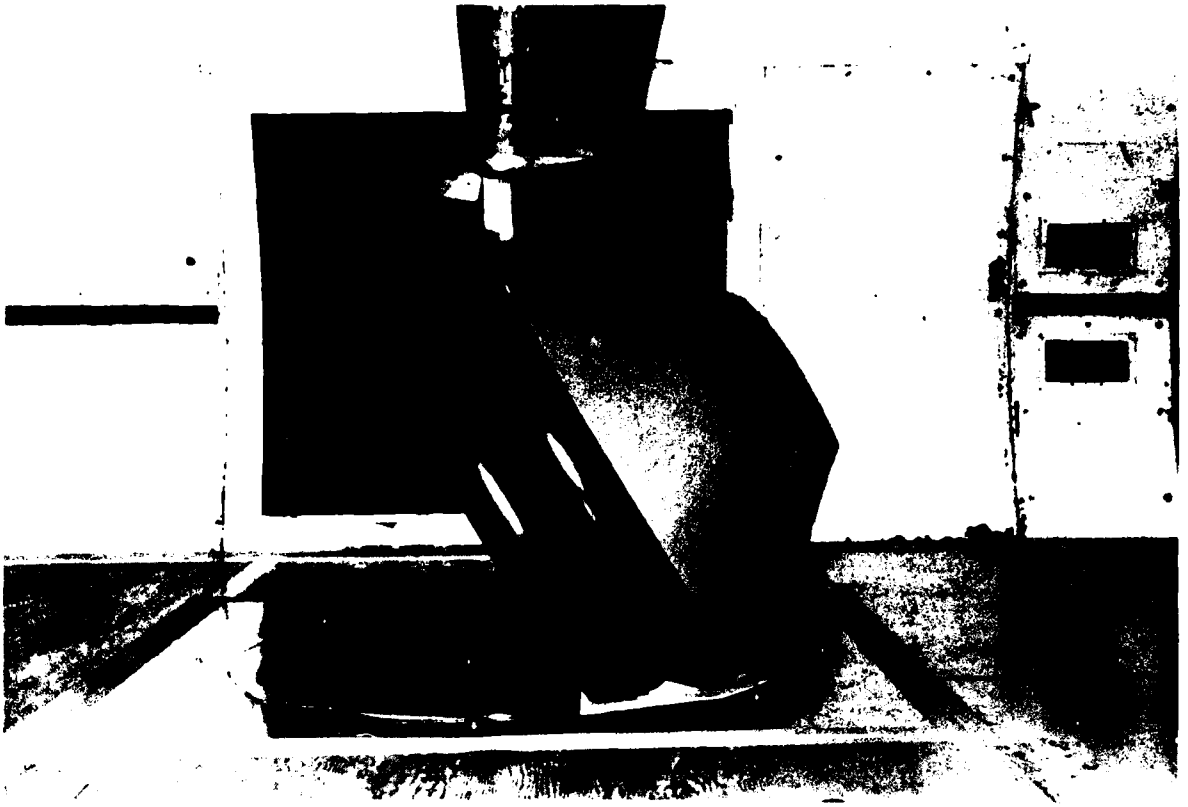

FIGURE 5-10

FLAT BOTTOM LIFERAFT CONFIGURATION AT

60 DEG. PITCH AND 18 PERCENT BOTTOM IMMERSION

FIGURE 5-11

FLAT BOTTOM LIFERAFT CONFIGURATION AT

20 DEG. PITCH AND 20 PERCENT BOTTOM IMMERSION

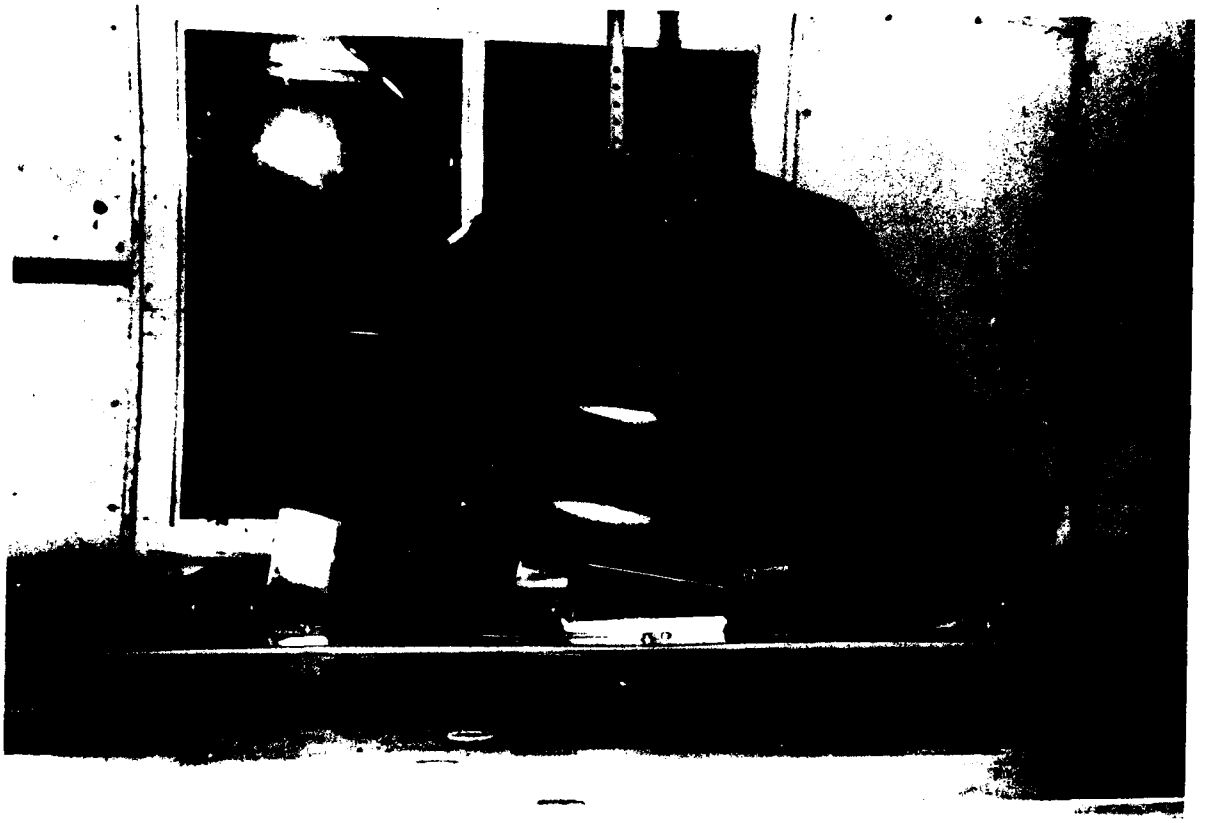

FIGURE 5-12

BALLAST POCKET LIFERAFT CONFIGURATION AT

10 DEG. PITCH AND 0 PERCENT BOTTOM IMMERSION

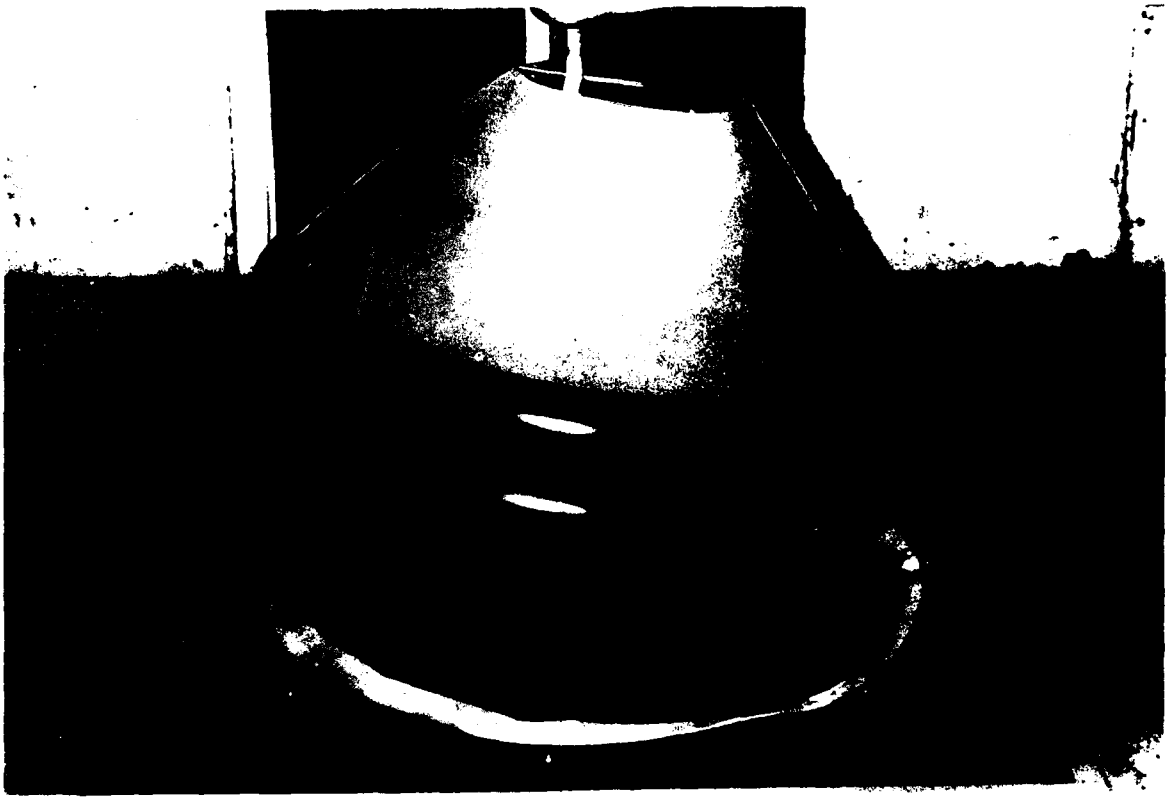

FIGURE 5-13

VIEW OF MODEL WITH THE HEMISPHERICAL BALLAST BAG

SUSPENDED OVER THE GROUNDBOARD CUTOUT

FIGURE 5-14

HEMISPHERICAL BALLAST BAG LIFERAFT CONFIGURATION

AT 30 DEG. PITCH AND 47 PERCENT BOTTOM IMMERSION

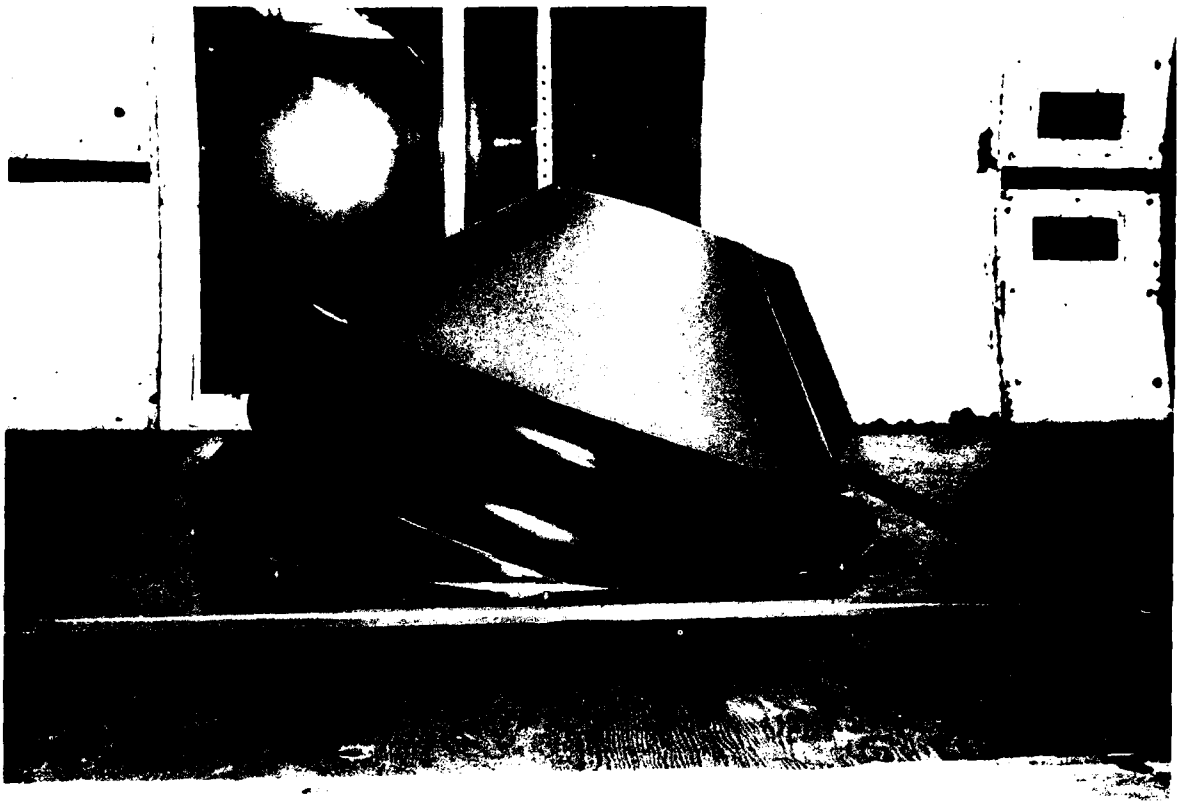

FIGURE 5-15

HEMISPHERICAL BALLAST BAG CONFIGURATION AT

20 DEG. PITCH AND 47 PERCENT BOTTOM IMMERSION

those for the hemispherical ballast bag configuration. Figure 5-16 shows the model with the toroidal ballast bag at 20 degrees and d' at 46 percent of D. The similarity of the above water geometry with the hemispherical ballast bag model in the same condition in Figure 5-15 should be noted.

The toroidal ballast bag configuration was also tested at 40 degrees pitch angle and with d' at 50 percent of D. This is an unrealistic condition because the low side of the raft is well swamped and the buoyancy is insufficient to support the weight of ballast water. This condition was tested to determine the character of the aerodynamic forces and moment when the underside of the toroidal ballast bag is exposed to the wind. The model in this condition is shown in position in the wind tunnel test section in Figure 5-17. In Figure 5-18, the model is shown suspended above the groundboard cutout. Thd difficulty in fabricating the groundboard seal is evident from the photo and is responsible for this one test condition absorbing about 20 percent of the total testing time.

5.4 Test Results

A complete tabulation of the lift, drag, and moment coefficients for all of the tests is given in Table 5-1. There are 17 data points to describe the dependance of the aerodynamic coefficients on pitch angle and bottom immersion. Within this set of data there is one set that includes all angles at approximately the same value of d' (20 percent of D) and two sets that includes the complete range of d' (from zero to 100 percent of D) at a single angle (10 and 20 degrees). The condition at 100 percent of bottom immersion was only tested at zero degrees pitch angle. It is expected that there is little change in the lift force as the pitch angle changes with full bottom immersion while the drag force should reduce as approximately the cosine of the pitch angle. Large angles with full bottom immersion are unrealistic (for the purpose of the quasi-static stability model) since this would require that the low end of the raft would be swamped.

A complete definition of aerodynamic coefficients throughout the range of interest of pitch angles and for all bottom immersions from zero to full is required for complete evaluation of the stability of an inflatable liferaft by means of the quasi-static model. To obtain this from the limited wind tunnel test results available, the data were cross-faired to produce families of curves. The

FIGURE 5-16

TOROIDAL BALLAST BAG CONFIGURATION AT

20 DEG. PITCH AND 46 PERCENT BOTTOM IMMERSION

FIGURE 5-17

TOROIDAL BALLAST BAG CONFIGURATION AT

40 DEG. PITCH AND 50 PERCENT BOTTOM EXPOSURE

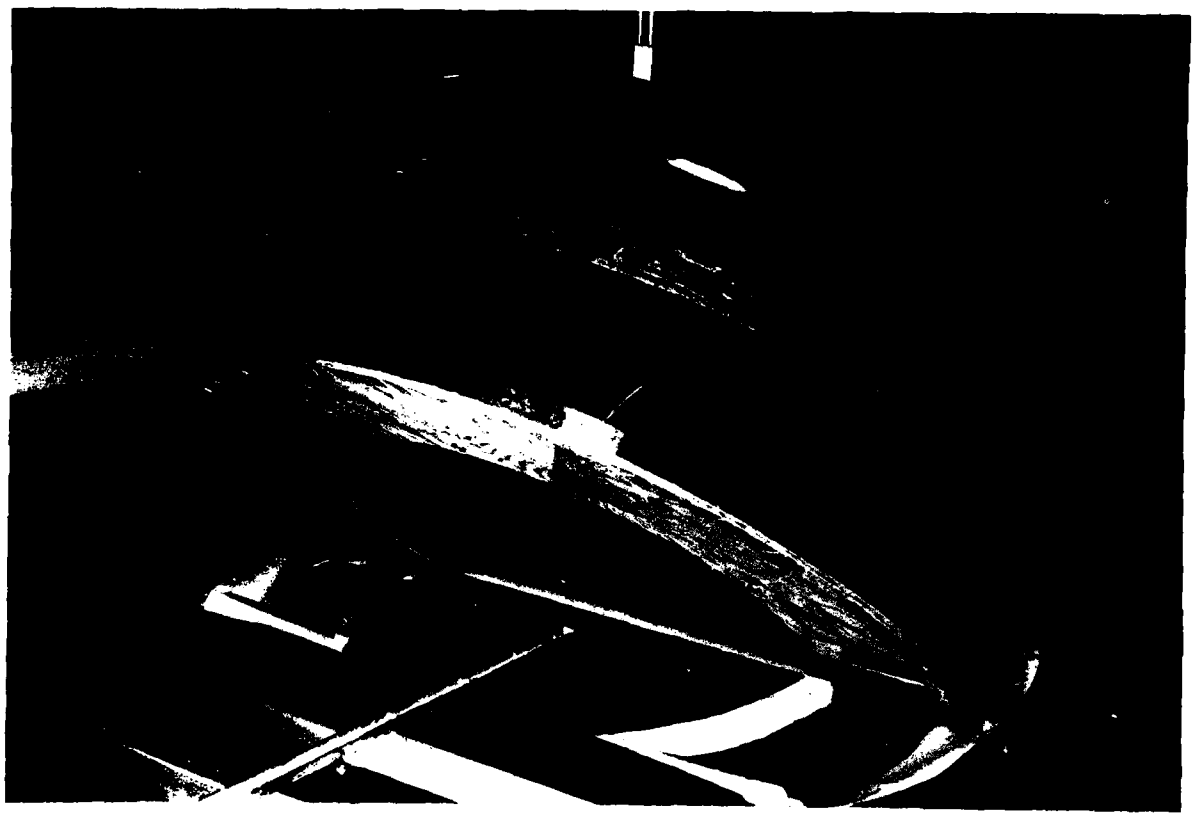

FIGURE 5-18

VIEW OF MODEL WITH TOROIDAL BALLAST BAG SUSPENDED

OVER GROUNDBOARD WITH CUTOUT FOR 40 DEG., 50 PERCENT CONDITION

TABLE 5-1

INFLATABLE LIFERAFT WIND TUNNEL TEST RESULTS

RUN NO.	CONFIGURATION	PITCH ANGLE, θ, DEG.	BOTTOM IMMERSION d'/D	C_L	C_D	C_M
3	Flat Bottom	0	1.0	0.288	0.269	0.020
4	Flat Bottom	30	0	1.042	0.748	-0.213
5	Flat Bottom	20	0	0.966	0.654	-0.173
6	Flat Bottom	10	0	0.972	0.473	-0.135
7	Ballast Pockets	30	0	0.990	0.722	-0.212
8	Ballast Pockets	20	0	0.963	0.644	-0.194
9	Ballast Pockets	10	0	0.981	0.462	-0.132
10	Flat Bottom	0	0	-0.217	0.259	-0.177
11	Flat Bottom	40	.12	1.212	0.832	-0.390
12	Flat Bottom	30	.18	1.367	0.635	-0.477
13	Flat Bottom	20	.20	1.398	0.506	-0.423
14	Flat Bottom	60	.18	1.011	0.912	-0.651
15	Flat Bottom	50	.28	1.184	0.769	-0.677
16	Flat Bottom	40	.44	1.048	0.561	-0.469
17.	Flat Bottom	30	.46	1.119	0.471	-0.376
18	Flat Bottom	20	.49	0.998	0.379	-0.208
19	Flat Bottom	10	.51	0.863	0.309	-0.020

TABLE 5-1 (con't)

INFLATABLE LIFERAFT WIND TUNNEL TEST RESULTS

RUN NO	CONFIGURATION	PITCH ANGLE θ, DEG.	BOTTOM IMMERSION d'/D	C_L	C_D	C_M
20	Flat Bottom	10	.23	1.253	0.453	-0.261
21	Flat Bottom	10	.59	0.698	0.237	0.032
22	Flat Bottom	20	.63	0.770	0.292	-0.091
23	Hemispherical Ballast Bag	10	.45	0.314	0.340	-0.067
24	Hemispherical Ballast Bag	20	.47	0.284	0.438	-0.113
25	Hemispherical Ballast Bag	30	.47	0.323	0.333	-0.106
26	Hemispherical Ballast Bag	20	.68	0.304	0.243	-0.070
27	Hemispherical Ballast Bag	30	.62	0.449	0.237	-0.210
28	Toroidal Ballast Bag	40	.50	1.191	0.277	-0.579
29	Toroidal Ballast Bag	20	.46	0.645	0.346	-0.232
30	Toroidal Ballast Bag	20	.68	0.667	0.212	-0.293

curves of lift, drag, and moment coefficients produced by this method are shown in Figure 5-19, 5-20, and 5-21 respectively. The drag coefficient data has been approximated by a single equation:

$$C_D = 0.10 + (0.23 + 0.0179\theta - 0.000866\theta^2)(1 - d'/D) + 0.17(d'/D)^5$$

where θ is the pitch angle in degrees.

The lift, drag, and moment coefficients for the ballast pocket configuration in the three conditions that were tested differed by an average of 3.1 percent from the coeffients for the flat bottom configuration. Since the three conditions were all for d' of zero, the ballast pockets had maximum exposure and it is reasonable to assume that the aerodynamic coefficients are essentially the same for all values of pitch and bottom immersion. Figures 5-19, 5-20, and 5-21 are therefore assumed to be valid representations of the lift, drag, and moment coeffients, respectively, for liferafts with ballast pockets provided that ballast pockets do not greatly exceed the proportions of those on the model (i.e. depth about equal to the tube diameter).

The results of the tests of the hemispherical ballast bag configuration in five conditions did not exhibit any discernable trend of the lift coefficient with either pitch angle or length of bottom immersion. This is more or less what would be expected since the entire raft with the ballast bag is somewhat like a whole sphere and therefore has about the same shape whatever the orientation. The lift coefficient is therefore taken as constant at the apparent average value of 0.30 for all values of pitch and bottom immersion. The drag coefficient appears to follow the curve for 10 degrees pitch angle of the flat bottom configuration. Accordingly, the drag coefficient for the hemispherical ballast bag is given by the equation:

$$C_D = 0.10 + 0.40\ (1 - d'/D) + 0.17(d'/D)^5$$

for all values of pitch angle. No trend of the moment coefficient with either pitch angle or bottom immersion was evident from the results of the limited number of conditions tested. The moment coefficient for the raft with the hemispherical ballast bag is therefore taken as constant at the average value of -0.10 for all pitch angles and bottom immersion.

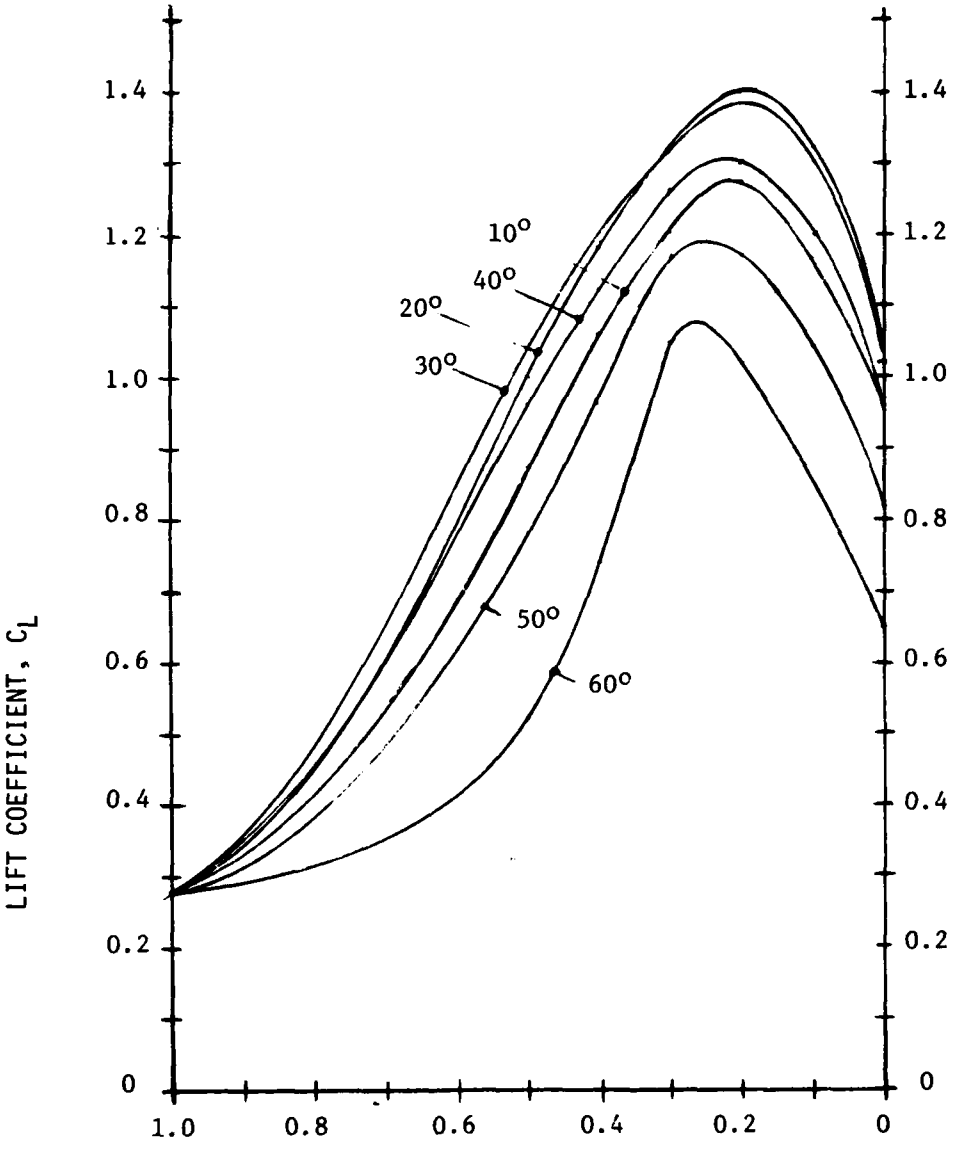

FIGURE 5-19

CURVES OF LIFT COEFFICIENT, C_L, VERSUS BOTTOM IMMERSION, d'/D, AND PITCH ANGLE, θ, FOR FLAT BOTTOM (UNBALLASTED) AND BALLAST POCKET INFLATABLE LIFERAFTS

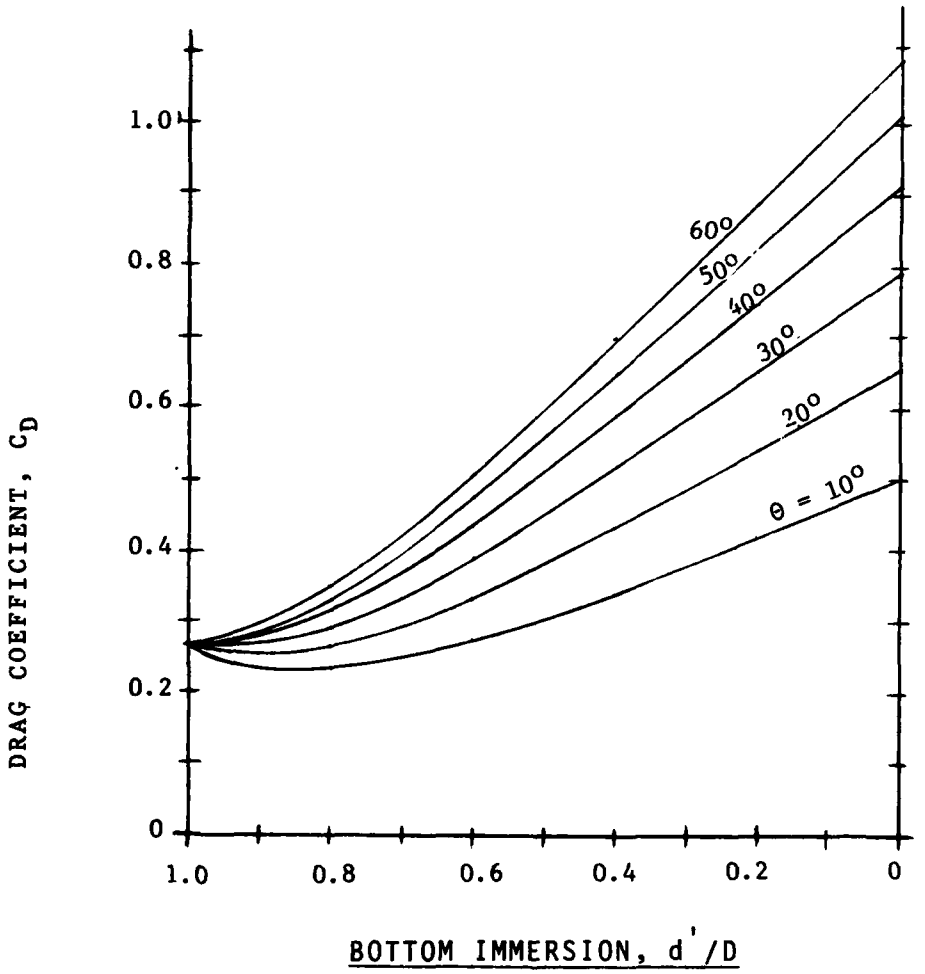

FIGURE 5-20

CURVES OF DRAG COEFFICIENT, C_D, VERSUS BOTTOM IMMERSION, d'/D, AND PITCH ANGLE, θ, FOR FLAT BOTTOM (UNBALLASTED) AND BALLAST POCKET INFLATABLE LIFERAFT CONFIGURATIONS

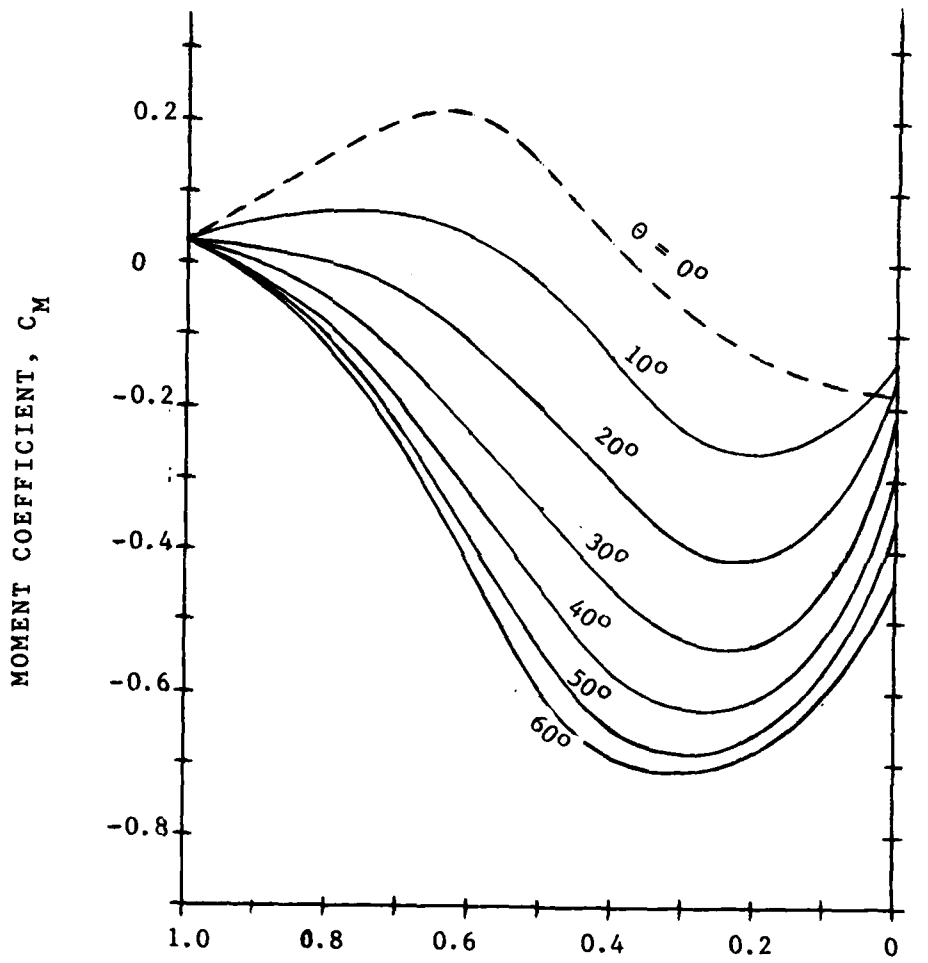

FIGURE 5-21

CURVES OF MOMENT COEFFICIENT, CM, VERSUS BOTTOM IMMERSION, d'/D, AND PITCH ANGLE, θ, FOR FLAT BOTTOM (UNBALLASTED) AND BALLAST POCKET INFLATABLE LIFERAFT CONFIGURATIONS

The toroidal ballast bag configuration was tested at only one angle (with the bottom of the ballast bag fully immersed) which precludes the development of any trend of aerodynamic coefficients with pitch angle. Nevertheless, as discussed above, it was expected that, as long as the bottom of the ballast bag remained immersed, the coefficients would be about the same as for the hemispherical ballast bag coefficients. This was borne out except that the constant lift coefficient value was about double at 0.65 and the constant moment coefficient value is also about double at -0.26.

When the bottom of the toroidal ballast bag was exposed in the 40 degree pitch angle test condition, the lift coefficient increased considerably, as expected, to 1.19. This is 24 percent greater than the flat bottom configuration at the same angle and bottom exposure. In the absence of test results at other pitch angles and extent of bottom exposure, the best estimate of the trend of lift coefficient with pitch angle and bottom immersion is that it follows the trend of the flat bottom coefficients. Thus, when the combination of pitch angle bottom exposure and toroidal ballast bag geometry results in the bottom of the ballast bag becoming exposed, the lift coefficient is taken as 1.24 times the lift coefficient for the flat bottom configuration. This seems reasonable since the inside of the toroid forms a cup to catch the wind creating high pressures under the liferaft much like an anemometer cup is designed to do. Until the bottom becomes emerged, the drag coefficient for the toroidal ballast bag configuration follows the trend for the hemispherical ballast bag configuration, i.e.

$$C_D = 0.10 + 0.40(1 - d'/D) + 0.17(d'/D)^5$$

The moment coefficient of the toroidal ballast bag configuration when the bottom was exposed in the 40 degree pitch angle test condition was -0.58. This is about 30 percent greater than the flat bottom configuration in a similar condition. In the absence of additional test data, the moment coefficient for the toroid is assumed to be uniformly 30 percent greater than the flat bottom whenever the bottom is exposed.

6.0 WAVE TANK TESTS

The Quasi-Static Inflatable Liferaft Stability Model provides a measure of the inherent stability characteristics of particular liferaft configurations. The model by itself, however, cannot predict the tendency of a particular liferaft to capsize at sea under specific wind and wave conditions because signigicant dynamic forces are in effect which are omitted from the model. The model has utility for this purpose if there can be shown to be a correlation between capsizing tendency at sea and the value of the stability measure as determined by the Quasi-Static Model.

To accomplish this, liferaft models were tested in wind and waves at the Offshore Technology Corporation at Escondido, California. Models of liferafts with the four ballast configurations and with a skirt configuration were tested to observe their tendency to capsize. No instrumentation was fitted in the models and no measurements were taken.

6.1 Test Plan

The plan called for the model to be subjected to increasingly severe wind and wave conditions until a condition was reached where the model capsized repeatedly. Other liferaft configurations would be judged to be more or less stable depending on whether they exhibited a tendency to capsize in more or less severe wind and wave conditions. For this test procedure to produce the desired results it is essential that at least the less stable models be capsized in the test tank for if no models were capsized, it would not be possible to infer that one were more stable than another.

Wind was produced by a 50 H.P. axial fan mounted about four feet above the water surface on the centerline of the tank. Wind velocity averaging 17.8 knots over the 20 ft. long test area and with a peak velocity of 19.5 knots at the center of the test area, measured six inches above the still water surface, was generated in the direction of wave propagation. Since this wind velocity is fairly low in terms of scaled full scale wind velocities that could cause capsizing,

the maximum wind was used for all tests. The same 3 foot, 0 inche diameter liferaft model that was used for the wind tunnel tests was used in the initial wave tank tests.

Preliminary calculations based upon preliminary British wind tunnel test results and a preliminary version of the Quasi-Static Stability Model indicated that the three foot diameter model in the light load condition would be unstable at 30 degrees pitch angle in a 19 knot wind. This was verified at OTC by holding the model at 30 degrees in the wind field, with no waves but buoyantly supported, then suddenly releasing it. The model was readily capsized from this position which verified that the preliminary calculation were correct in determining the model to be unstable in the available wind conditions when the bottom became exposed to the extent consistent with the pitch angle and loading condition.

The next step in the test procedure was to determine the sea state which was just sufficient to cause the model to capsize (with the same wind velocity as in the previous step). To save time in testing in sea states which would be insufficient to cause capsizing the model was first tested in the largest waves which could be generated at OTC. The wave height would then be reduced in steps until a condition was reached at which the model could not be capsized. Regular waves were generated so that the exact characteristics of the wave which caused capsizing would be known.

The least stable configuration of the model, i.e. the flat bottom (Unballasted) configuration in its lightest load condition was tested in 28 inch regular waves with a 2.2 second period. The model was allowed to drift without external constraints through the area of maximum wind velocity. The model had no tendency to capsize. The model was observed to contour the regular waves very closely. Although the model achieved angles up to 20 degrees as it rode on the surface of the waves, the bottom never became exposed as it would if it were pitched at that angle in smooth water and therefore wind lift forces were not developed. Even as the liferaft model rode over the crests of the waves, no more than 10 or 15 percent of the bottom would become exposed. Smaller regular waves with shorter lengths were tried with the same result. This behavior of the liferaft in regular waves is consistant with the high static stability of the shallow, cir-

cular liferaft hull form and the fact that the resultant inertial force vector is normal to the water surface of a regular trachoidal wave.

Testing was terminated to construct a smaller model. At this point, the Cal Tech wind tunnel test results were available and the Quasi-Static Stability Model was more fully developed to permit a more accurate estimate of the stability of a liferaft configuration. Calculations confirmed the earlier estimate that the 3 foot diameter model would be unstable in a 20 knot wind at 30 degrees pitch in the light load condition with 65 percent of the bottom exposed. Calculations also showed that an 18 inch diameter model would be unstable at ten degrees in the light load condition but would be stable through thirty degrees in the full load condition. Thus, the calculations indicate that the failure of the three foot model to capsize was due to the absence of relative pitch motion in regular waves. Since the dynamic analysis of liferaft motions in waves was precluded from the scope of this study, it was not possible to determine apriori whether any wave conditions could be generated at the OTC tank which could cause the amount of pitch angle and bottom exposure which could cause capsizing as predicted by the Quasi-Static Model. Therefore in the next series of wave tank tests, an 18 inch diameter model was to be tested in the most severe irregular sea static available at the tank to improve, the likelihood that capsizes would occur.

The 18 inch diameter model was identical in all proportions to the 36 inch diameter model. The tubes of this model were made from rubber inner tubes (instead of foam as in the 36 inch model) but the model was made as rigid as the larger model by a combination of high air pressure and a solid foam core.

The model in the various ballast configurations was tested in a long crested, irregular Pierson-Moskowitz sea spectrum with a significant wave height of 16 inches. Each time the sea state was generated the same sequence of irregular waves was repeated. This ability to repeat the same random sea sample has two advantages for the test program. First, when a capsizing of a model does occur, it is possible to repeat the event to ensure that a definite capsizing mechanism was in fact operational in that part of the spectrum. Second, it ensures that all of the various model configurations are tested under identical conditions.

This insures that conclusions drawn regarding the relative performance of alternative configurations relate solely to differences in the configurations and not also to differences in the simulated environmental conditions.

6.2 Test Results

The principal result of the test of each model configuration was the determination of whether there was a repeatable tendency of the model to capsize. The test of each configuration in the sea state was repeated until a firm conclusion could be reached. If capsizing could be repeated three or four times in succession, the configuration was judged to be definitely capsizable. If it only capsized once or twice in several attempts it was judged marginally capsizable and if it never capsized in several attempts it was judged to have no tendency to capsize. A summary of all tests is given in Table 6-1.

A 16 mm color film of all significant events is furnished with this report. In general, after a tendency to capsize had been established, the event was repeated for filming. Configurations which had no tendency to capsize and/or demonstrated high degrees of stability by their motion response were filmed for relatively longer durations to record these tendencies.

6.2.1 Flat Bottom (Unballasted) Configuration: Wave Tests

The model in the flat bottom, unballasted configuration in the light load condition (i.e. 2.25 lbs., corresponding to an empty, 109 lb., full scale six man liferaft) was repeatedly capsized in the two largest waves of the 10 minute wave record, both with and without the 19 knot wind blowing. Both of these waves which caused the model to capsize were breaking. The model did not show any tendency to capsize in any other waves in the entire generated sea state although many of these waves were also breaking.

Figure 6-1 and 6-2 show the model in the process of being overturned in the breaking wave. In all other non-breaking waves the model performed as the three foot model did in regular waves, i.e. the model did not expose the bottom by pitching out of phase with the wave surface. This is illustrated in Figure 6-3

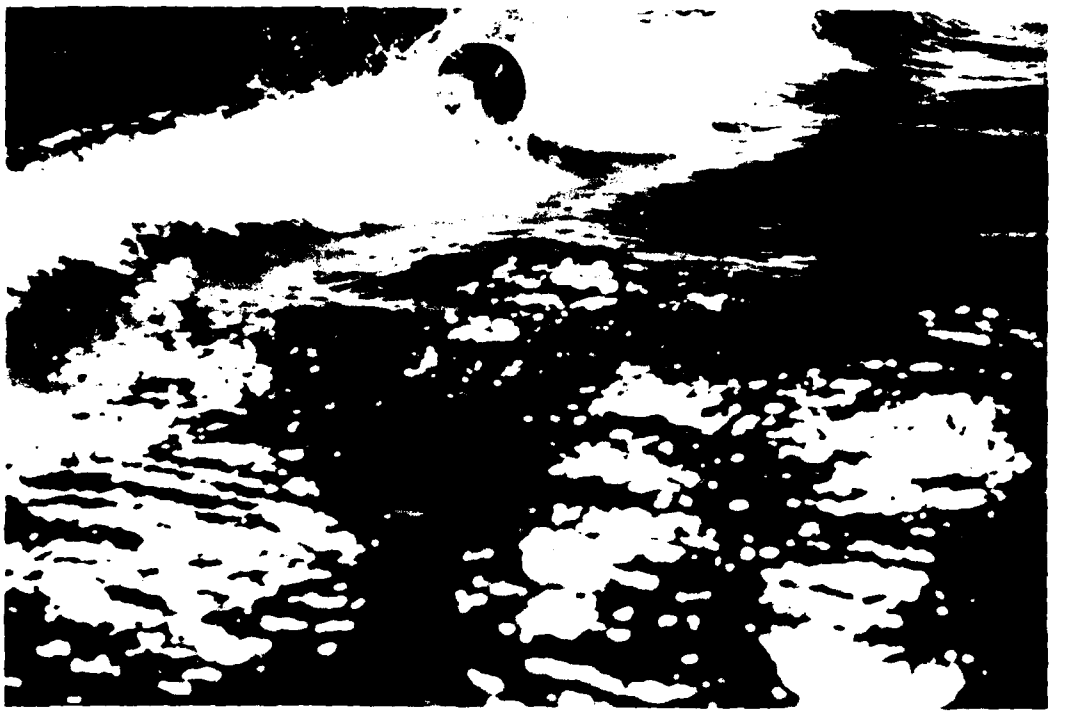

FIGURE 6-1

FLAT BOTTOM (UNBALLASTED) LIFERAFT MODEL BEING

CAPSIZED IN A BREAKING WAVE WITH NO WIND

FIGURE 6-2

FLAT BOTTOM (UNBALLASTED) INFLATABLE LIFERAFT MODEL

BEING CAPSIZED IN A BREAKING WAVE WITH 19 KNOTS WIND

FIGURE 6-3

FLAT BOTTOM (UNBALLASTED) INFLATABLE LIFERAFT MODEL

RIDING OVER THE CREST OF A STEEP, BUT NON-BREAKING WAVE

TABLE 6-1

SUMMARY OF LIFERAFT TESTS IN WIND AND WAVES

CONFIGURATION	WEIGHT LBS.	WIND SPEED KNOTS	SIGNIFICANT WAVE HEIGHT	NO. OF CAPSIZIES
	2.25	19	16"	4
	2.25	0	16"	4
	2.25	0	(IMPULSE)	3
FLAT	2.25	19	13"	0
BOTTOM	2.25	19	10"	0
(UNBALLASTED)	2.25	19	6"	0
18" MODEL	9.45	19	16"	7
	9.45	0	16"	4
	9.45	0	(IMPULSE)	1
	13.69	19	16"	2
	13.69	0	16"	1
	13.69	0	(IMPULSE)	2
FLAT BOTTOM (UNBALLASTED) 36" MODEL	20.0	19	16"	6
	20.0	0	16"	2
	4.48	19	16"	4
	4.48	0	16"	0
	4.48	0	(IMPULSE)	0
BALLAST	10.47	19	16"	3
POCKETS	10.47	0	16"	3
18" MODEL	10.47	0	(IMPULSE)	0
	15.8	19	16"	1
	15.8	0	16"	0
	15.8	0	(IMPULSE)	0
BALLAST POCKETS 36" MODEL	35.5	19	16"	0

TABLE 6-1 (con't)

CONFIGURATION	WEIGHT LBS.	WIND SPEED KNOTS	SIGNIFICANT WAVE HEIGHT	NO. OF CAPSIZIES
TOROIDAL	25.0	19	16"	0
BALLAST	25.0	0	(IMPULSE)	0
BAG	31.0	19	16"	0
18" MODEL	31.0	0	(IMPULSE)	0
TOROIDAL BALLAST BAG 36" MODEL	N.A	19	16"	0
HEMISPHERICAL	47.5	19	16"	0
BALLAST BAG	54.5	19	16"	0
18" MODEL	54.5	0	(IMPULSE)	0
HEMISPHERICAL BALLAST BAG 36" MODEL	N.A	19	16"	0

where the model is shown riding flat on the surface of a rather steep, but non-breaking wave. The 3 foot model was also capsized in the largest wave in this sea state as shown in Figure 6-4 although the capsize could not always be repeated.

In the irregular sea state, breaking waves were created when large, fast moving waves catch up with smaller, slow moving waves and the crests are superimposed to produce steeper waves than can be produced singly. When a steep wave is produced in this manner which is steeper than can be sustained, the unstable crest collapses. The faster moving wave passes beyond the slower wave and the crest flattens out. Thus, the breaking crests occur sporadically throughout the generated sea state. The wave which caused the liferaft model to capsize was the largest one that was produced by the wave generator at the test position in the tank. Equally large breaking waves may, and probably did, occur at other locations in the tank. Some flexibility was available within the test area to position the model at the exact location where it was known that the wave would break. The position of the model was somewhat critical to whether the breaking wave would capsize the model or not. If the model were positioned where the wave was just starting to break or where the breaking crest was already collapsed, the model very often rode through the wave without capsizing. This effect was most pronounced with the 3 foot diameter model which appeared to only capsize if the breaking wave passed the model when the forward vector of the collapsing crest was strongest.

Although there were only a limited number of opportunities for the model to encounter a critical wave at the critical point in time (or space) in the tank test, there are many more opportunities for the event to occur during the duration of an actual storm at sea. Thus, if a liferaft in a particular configuration can be shown to capsize in the test tank, then it will probably capsize under the same conditions at sea.

In addition to the long crested irregular seas, the model was also tested in a single breaking wave which is produced by generating a succession of regular waves of increasing height and at such intervals that they all reach a point in the length of the tank at the same time with all crests superimposed. There

FIGURE 6-4

THREE FOOT DIAMETER MODEL OF FLAT BOTTOM INFLATABLE LIFERAFT CONFIGURATION BEING CAPSIZED IN A BREAKING WAVE WITH 19 KNOTS WIND

was no wind in the area where this test was conducted. The 18 inch flat bottom (unballasted) liferaft in the light load condition was as easily capsized by this breaking wave as by the irregular sea, however, the wave slope appeared to be less severe because the wave did not have the deep trough of a preceding wave in front of it.

The fact that the model was as easily capsized without wind as with wind in breaking waves suggests that there is a mechanism for capsizing that is entirely separate from the capsizing due to wind forces as developed mathematically in the Quasi-Static Inflatable Liferaft Stability Model. Nevertheless visual observations indicate that capsizings initiated in breaking waves are often completed by the wind force. Figure 6-5 shows the raft still upright after the breaking wave has passed under it. The bottom is about 85 percent exposed with the wind field (visible on the water surface upstream of the raft) acting on it to complete the capsize.

The model in the flat bottom (unballasted) configuration was tested in three loading conditions. Even in the full load condition at 13.7 lbs. (where the Quasi-Static Stability Model shows the raft to be stable through 30 degrees pitch angle), the model was easily capsized with and without wind in breaking waves.

The flat bottom (unballasted) liferaft model was also tested in the least stable light load condition in the same Pierson-Moskowitz sea spectrum at progressively lower significant wave heights of 13 inch, 10 inch, and 6 inch and it was not possible to capsize the raft. This suggests that there are nonlinear scale effects involved in the dynamic capsizing mechanism since if there were a linear effect, the 18 inch model would capsize in an 8 inch sea state in the same way that the 36 inch model capsized in the 16 inch sea state.

6.2.2 Ballast Pocket Configuration Wave Tests

The model with the ballast pockets fitted showed about the same tendency to capsizing as the model without any ballast at all. A notable exception was the failure of the model to capsize in the empty load condition with no wind although

FIGURE 6-5

FLAT BOTTOM (UNBALLASTED) INFLATABLE LIFERAFT MODEL PITCHED UP, BUT NOT CAPSIZED, BY BREAKING WAVE IN THE PROCESS OF BEING CAPSIZED BY THE 19 KNOT WIND

it capsized three times in the same conditions in the more stable half load condition. (It is suspected that the critical positioning factor referred to earlier may have been the cause of this apparent anomaly.)

Another difference was that the model with ballast pockets did not capsize in the impulsive breaking wave in any load condition whereas without ballast pockets, it was capsized in that wave in every load condition. Also the 36 inch diameter model did not capsize in the same wind and wave conditions in which the 36 inch model without ballast was capsized.

The overall conclusion that can be drawn from a comparison of the wind and wave tests of the ballast pocket and the unballasted liferaft configurations is that the ballast pockets do not greatly reduce the tendency to capsize but where the tendency was marginal in the unballasted case, ballast pockets do appear to make some positive difference. It would have been interesting to have comparative results with ballast pockets of about twice the size. It should be realized, however, that as ballast pockets are made progressively larger, their ends would tend to come together around the quadrents so that they would ultimately become toroidal ballast bags.

Figure 6-6 shows the model with ballast pockets having been capsized by a breaking wave. Note that the breaking wave has already collapsed and the model has completed its capsize but is on the forward edge of the wave (which is advancing from left to right). This indicates that the model has been tossed forward by the breaking wave.

6.2.3 Toroidal Ballast Bag Configuration Wave Tests

The toroidal ballast bag configuration of the liferaft model was tested in the empty and half load conditions in the 16 inch significant wave height Pierson-Moskowitz spectrum with 19 knots wind and with no wind in the impulsive breaking wave. The model did not show any tendency to capsize. Indeed, the model, in both load conditions, appeared to be so stable that immediately after crossing over the crest of a wave, whether breaking or not, it tended to return from the wave slope angle with a sharp, jerky motion. The 3 foot diameter model was

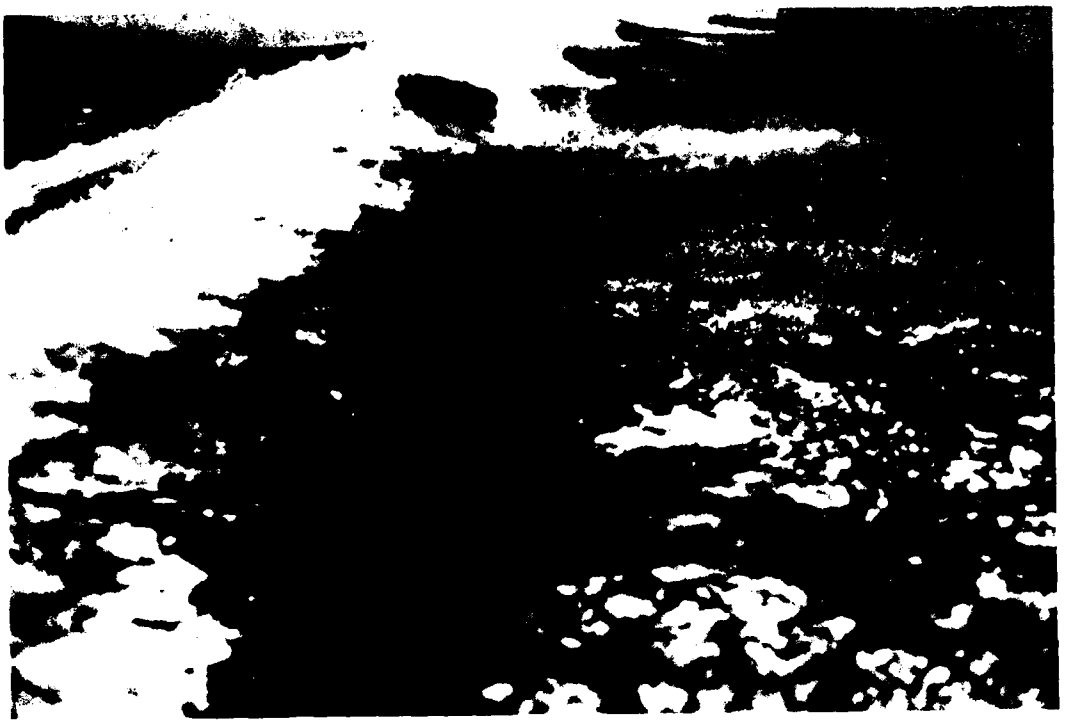

FIGURE 6-6

MODEL WITH BALLAST POCKETS CAPSIZED BY BREAKING WAVE

also tested in the light load condition and showed the same general behavior.

Figure 6-7 shows the model with the toroidal ballast bag passing through a large breaking wave with very little pitch excitation.

6.2.4 Hemispherical Ballast Bag Configuration Wave Tests

The hemispherical ballast bag configuration of the liferaft was tested in the empty and half load conditions in the 16 inch significant wave height Pierson-Moskowitz spectrum with 19 knots wind and in the impulsive breaking wave with no wind. The performance of the model was essentially the same as the toroidal ballast bag configuration. The model showed no tendency to capsize in any kind of wave. It also exhibited the same sharp, jerky response in going over the wave crests that the toroidal ballast bag configuration had. The 3 foot diameter model was also tested in the light load condition and showed the same general behavior.

Figure 6-8 shows the model with the hemispherical ballast bag passing through a breaking wave with very little pitch excitation.

6.2.5 Skirt Configuration Wave Tests

An attempt was made to test the model with a skirt configuration in accordance with the patent disclosure of Masami Hashimoto. The skirt was constructed of a sheet of polypropylene material attached to the bottom of the raft. The circular sheet extended 9 inches beyond the sides of the raft and floated on the surface.

It was not possible to determine the stabilizing performance of skirts with this model because wave action caused the skirt to become folded under the raft. Further design development appears to be needed to provide some means to assure that the skirt will remain extended, as it is intended to be, under severe sea conditions.

AD-A091 966 CASDE CORP TORRANCE CA F/G 6/7
INFLATABLE LIFERAFT STABILITY STUDY,(U)
SEP 79 F J NICKELS
DOT-CG-817775-A
UNCLASSIFIED USCG-D-81-79 NL

2 OF 2
AD A
091966

END
DATE FILMED
-81
DTIC

FIGURE 6-7

MODEL WITH TOROIDAL BALLAST BAG IN BREAKING WAVE

FIGURE 6-8

MODEL WITH HEMISPHERICAL BALLAST BAG IN BREAKING WAVE

6.2.6 Full Scale Raft: Wave Tests

A full scale six man raft was available and was scheduled to be tested during the first series of tests of the three foot diameter model. Due to the inability to capsize the half scale model at that time, it would have been pointless to attempt to test the full scale raft. For the same reason, the full scale raft was not included in the final series of tests.

7.0 ANALYSIS OF RESULTS

7.1 Righting Moment Curves

The Quasi-Static Inflatable Liferaft Stability Model was exercised to produce righting moment curves for all of the model configurations that were tested in the wave tank. The calculated stability is compared with the observed tank test performance to determine whether there is a correlation between calculated still water stability and performance in wind and waves and to provide a basis for formulation of stability criteria.

Figure 7-1 shows, as an example the calculated righting arm curve for the 18 inch model in the flat bottom, unballasted configuration and the light load (empty) condition, in zero wind speed. The Quasi-Static Model calculates the righting moment up to the angle at which the top of the upper buoyancy tube at the low side of the raft submerges. In Figure 7-1 this angle is 51 degrees and the righting arm curve is shown solid to that angle. Beyond that angle the evaluation of the righting moment becomes somewhat ambiguous because of uncertainty as to how the canopy maintains the watertight envelope. In the case shown in Figure 7-1, it can be deduced from the symmetry of the configuration (the assumed height of the center of gravity is at the juncture of the two buoyancy tubes) that the liferaft would have zero righting moment at 90 degrees pitch angle and so the righting moment curve is extended as a dashed line to that point.

Since the model in this configuration and load condition was readily capsized in waves, with and without wind, it can be concluded that the amount of righting moment shown in Figure 7-1 is inadequate to prevent capsizing. It would be incorrect to conclude that the heeling moment due to static and dynamic heeling forces exceeded 0.96 ft. lbs. to cause the raft to capsize since in the dynamic situation, the wave slope/pitch angle relationship alters the righting moment. All that can be reasonably concluded is that the raft with x amount of calculated stability capsized in certain wind and wave conditions.

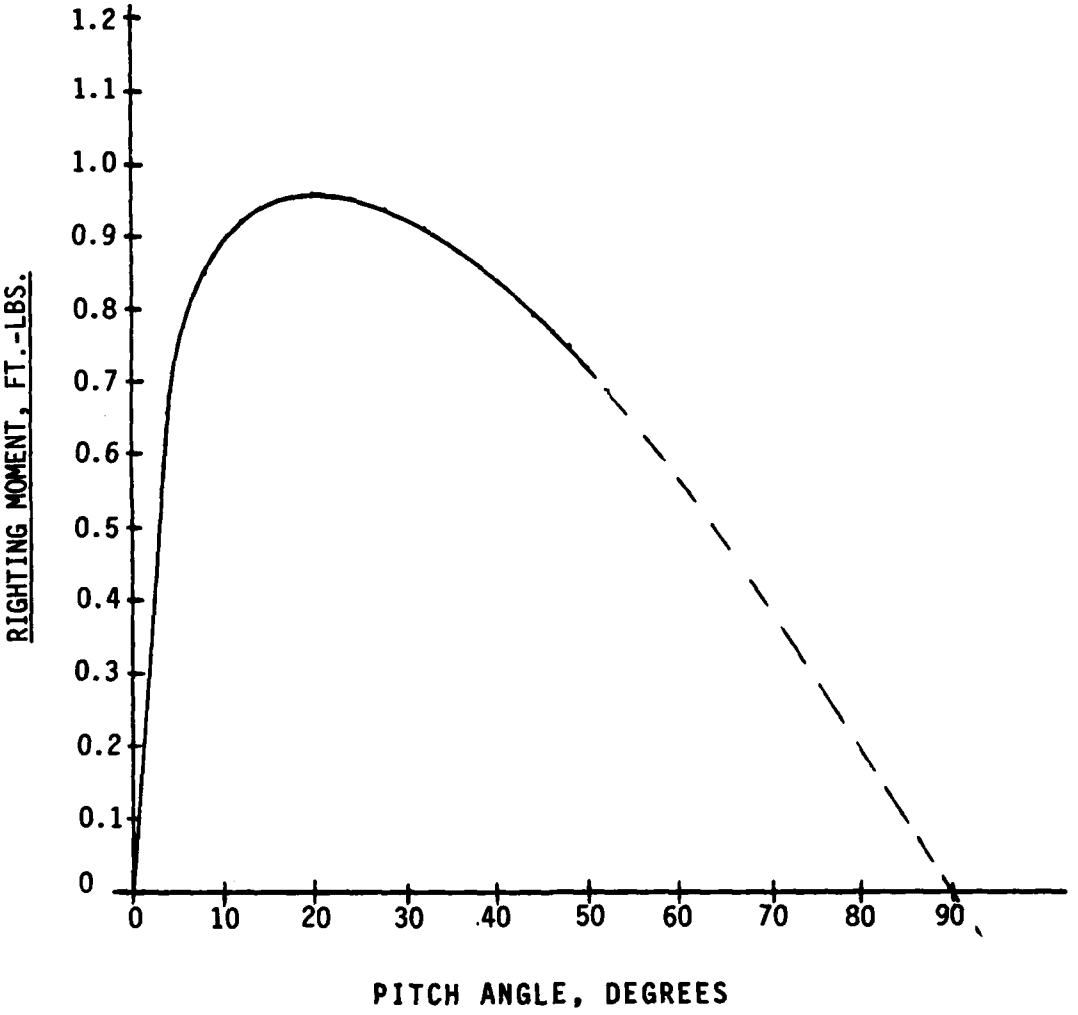

FIGURE 7-1

STILL WATER RIGHTING MOMENT CURVE FOR 18 INCH DIAMETER INFLATABLE LIFERAFT MODEL; FLAT BOTTOM (UNBALLASTED) CONFIGURATION; LIGHT LOAD (EMPTY) CONDITION; ZERO WIND SPEED

By comparing the righting moment curves of a wide variety of ballasted liferaft configurations in various load conditions with the tendency to capsize in standardized wind and wave conditions, a measure of adequate calculated still water stability which will prevent capsizing at sea may become evident. Since each configuration and load condition will have a different shape of righting moment curve, a standarized measure of stability derived from the specific righting moment curves is required. The maximum value of righting moment at whatever angle it occurs is probably the most meaningful measure of stability. A practical difficulty with using this measure is the inability of the Quasi-Static Model to calculate moments beyond the angle at which the upper buoyancy tube submerges. For the more heavily ballasted configurations, the maximum righting moment will occur beyond this angle.

Observation of model performance in wind and waves reveals, however, that configurations that do not capsize do not pitch much more than the wave slope. Therefore, evaluation of stability at fairly moderate pitch angles may be an equally meaningful measure of capsize resistance. As a tentative correlation of calculated still water stability with performance in waves the righting moment at 18 degrees has been selected because almost every configuration has a calculated value at that angle.

7.2 Comparison With Tank Test Results

Figure 7-2 shows the righting arm curves produced for the four ballast configurations in the light load (empty) condition with zero wind speed. At 25 degrees pitch angle, ballast pockets enhance the stability (over the flat bottom, unballasted configuration) by about 50 percent. The toroidal ballast bag configuration provides 6.5 times the stability of the unballasted configuration while the hemispherical ballast bag provided 5.5 times the stability. It should be noted that in this load condition at 25 degrees the bottom of the toroidal ballast bag has not yet emerged from the water. Beyond the angle at which it emerges, the righting moment of the toroidal ballast bag will start to decrease. On the other hand, as the pitch angle increases, the hemispherical ballast bag will tend to sag more which will significantly decrease the righting moment. It

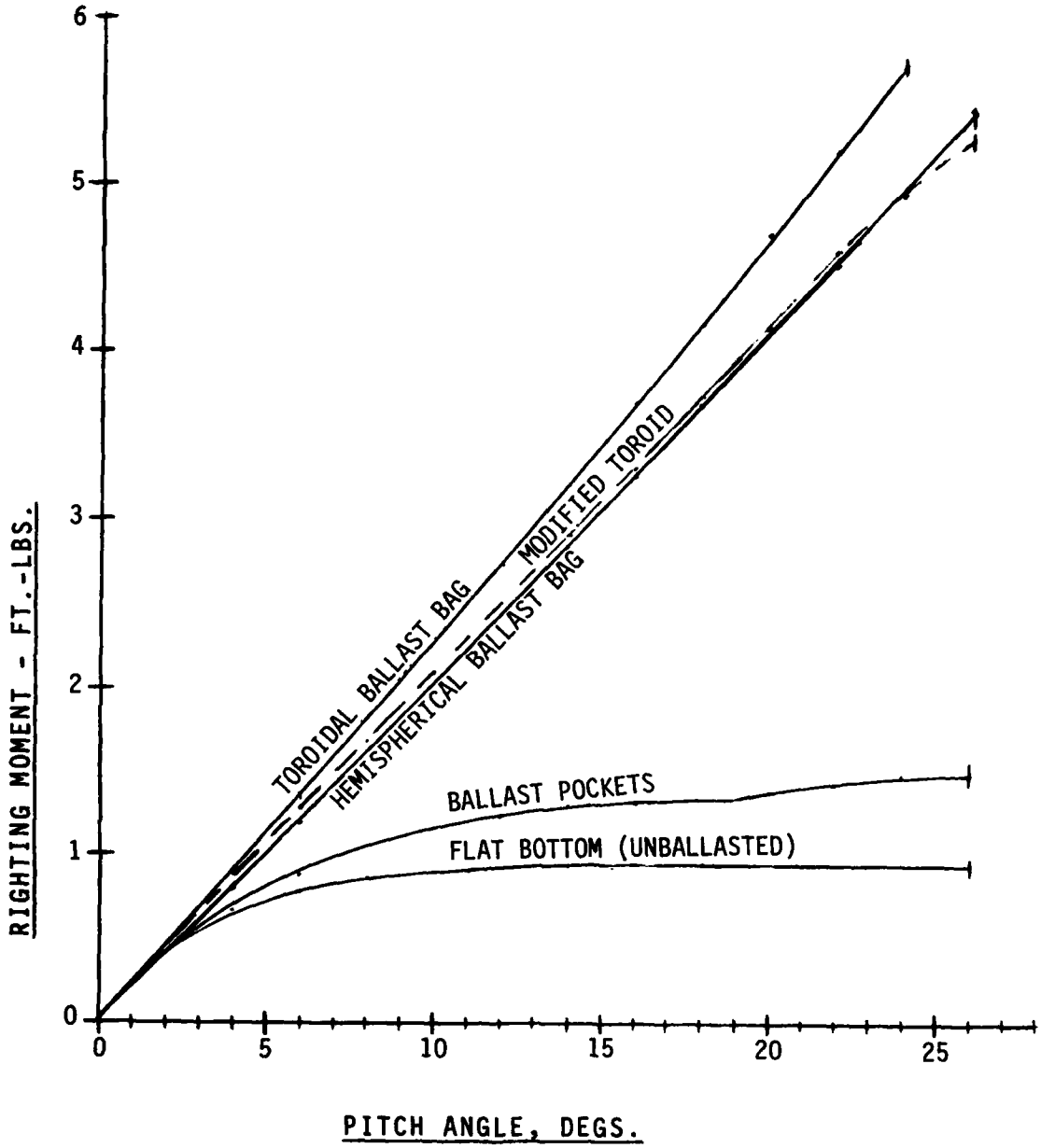

FIGURE 7-2

CURVES OF RIGHTING MOMENT FOR INFLATABLE LIFERAFTS WITH VARIOUS BALLAST CONFIGURATIONS WITH ZERO WIND

is therefore difficult to comparatively evaluate the stability of the hemispherical and toroidal ballast bag configurations at large angles under the simplifying assumptions adopted in this study. At small angles, the toroidal ballast bag concept appears to be superior.

Comparison of the calculated righting moment at 18 degrees pitch angle with the observed tendency of the model to capsize in wind and waves is made in Figure 7-3. There appears to be a clear demarkation between tendency to capsize and to stay upright for the 18 inch diameter model at a righting moment of 3.2 ft. lbs. Since the righting moment is proportional to the displacement times the righting arm, it varies as the fourth power of the linear dimension of the liferaft. On this basis the righting moment which prevents capsizing in the wind and wave conditions in which the model was tested could be generalized as a coefficient times D^4 ft. lbs. Based upon the results of the model tests, the coefficient would be 3.2 ft.-lbs./$(1.5\ ft)^4$ = 0.63 to yield a stability criterion of 0.63 D^4. However, it would be premature to apply such a measure as a general criterion for inflatable liferaft stability for several reasons.

First, the dynamic forces contributing to the heeling moment in a breaking wave undoubtedly vary in some other proportion of liferaft dimension. Since dynamic forces in breaking waves have been qualitatively demonstrated to be very significant to tendency to capsize, this factor cannot be ignored.

Second, the dynamic effects contributing to heeling moment in breaking waves are likely to be dependent upon underwater shape in addition to some simple linear dimension. Thus, the required righting moment to prevent capsizing may have to be specific to each configuration.

Third, the sea state in which the 18 inch model was tested scales linearly to sea state 4 for a 6 man liferaft and sea state 5 for a 25 man liferaft. A general stability criterion for inflatable liferafts should provide for resistance to capsizing in much higher sea states.

KEY:

× STRONG TENDENCY TO CAPSIZE

⊗ MARGINAL TENDENCY TO CAPSIZE

○ NO TENDENCY TO CAPSIZE

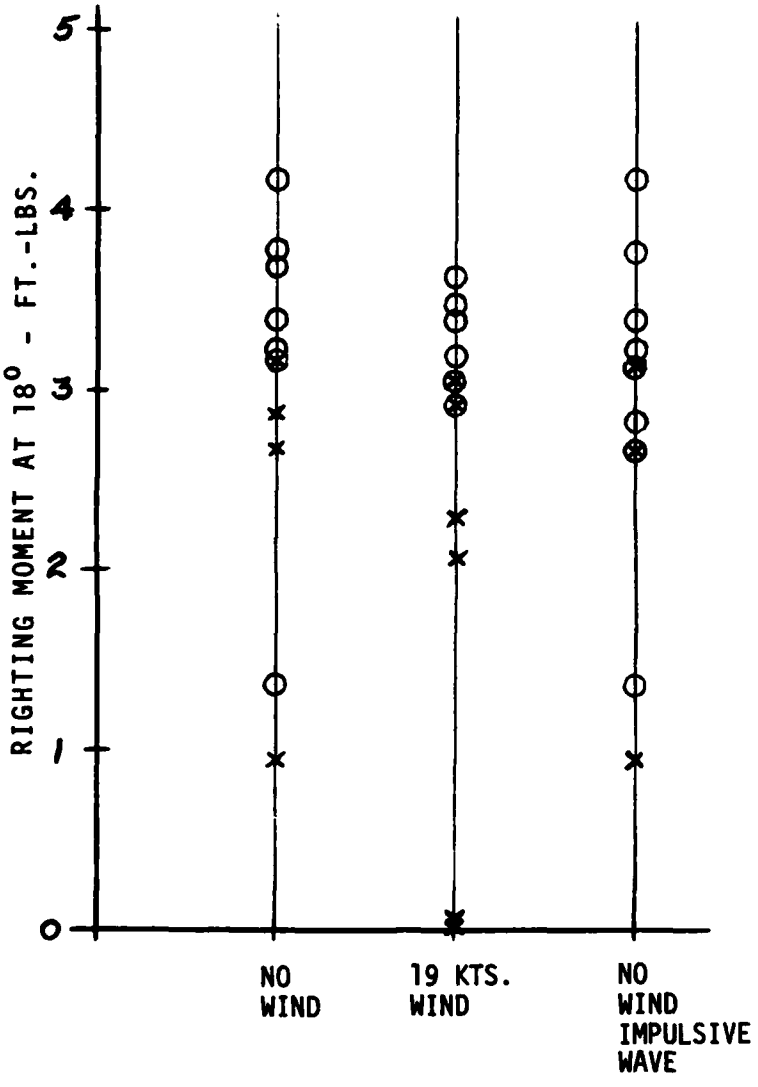

FIGURE 7-3

COMPARISON OF CALCULATED RIGHTING MOMENT

WITH OBSERVED TENDENCY TO CAPSIZE

7.3 Modified Toroid Configuration

It appeared in the wave tank tests that both the hemispherical and toroidal ballast bag configurations had excess stability. Neither showed the slightest tendency to capsize in any of the wave conditions imposed. That performance suggested that a smaller toroidal ballast bag might also provide adequate stability. Although the test schedule did not permit the construction and testing of an additional model, the righting moment was evaluated via the Quasi-Static Inflatable Liferaft Stability Model. The results are shown in Figure 7-2 with the dashed curve labeled "Modified Toroid". All dimensions for this configuration are the same as the toroidal ballast bag configuration that was tested except that the thickness of the ballast bag (i.e., the difference between the outer and inner radii) is halved so that there is approximately one half the weight of water.

At 18 degrees, the righting moment is reduced only 11 percent from 4.17 to 3.72 ft. lbs. and is still slightly greater than the 3.67 ft. lbs. of the hemispherical configuration yet the liferaft carries only one fourth the total weight of ballast water. It is expected that the modified toroidal configuration while providing adequate resistance to capsizing will also provide an easier ride in waves than the basic toroid or the hemispherical ballast bag configurations.

8.0 REFERENCES

1. Dayton, R.B., and Cornell, M.E.; Group Survival Equipment Effectiveness, Operations Research, Inc., January 1976.

2. Daniels, M.R., Jr., Markle, R.L., and Maness, S.G.; Preliminary Tests of Inflatable Liferafts for Stability in High Winds; U.S. Coast Guard, 1 December 1977.

3. Markle, R.L., Wehr, S.E., Daniels, M.R., and Maness, S.G.; Inflatable Liferaft Tests in the Pacific Ocean Off the Columbia River Bar; U.S. Coast Guard, 3 May 1978.

4. Petrie, G., and Walden, D.A.; A Time Domain Analysis of the Motion of a Disc Buoy in Breaking Waves; Hoffman Maritime Consultants Inc., May 1976.

5. Title 46, U.S. Code of Federal Regulations, Shipping.

6. Ponsford, P.J.; "A Wind-Tunnel Assessment of the Contribution of the Wind Loads on a Liferaft to the Problem of Overtuning", NMI TM26, National Maritime Institute, Feltham, Middlesex, UK, TW140LQ, November 1978. (unpublished)

*U S GOVERNMENT PRINTING OFFICE: 1980 720-509/5


DATE
ILME